BEHAVIOR OF FLEXURAL MEMBERS MADE FROM OIL PALM SHELL AND CLINKER CONCRETE

MD. NAZMUL HUDA

FACULTY OF ENGINEERING

UNIVERSITY OF MALAYA

KUALA LUMPUR

2017

BEHAVIOR OF FLEXURAL MEMBERS MADE FROM OIL PALM SHELL AND CLINKER CONCRETE

MD. NAZMUL HUDA

DISSERTATION SUBMITTED IN FULFILLMENT OF THE PARTIAL REQUIREMENTS FOR THE DEGREE OF MASTER OF ENGINEERING SCIENCE

FACULTY OF ENGINEERING
UNIVERSITY OF MALAYA
KUALA LUMPUR

2017

UNIVERSITY OF MALAYA

ORIGINAL LITERARY WORK DECLARATION

Name of Candidate: **Md. Nazmul Huda**

Passport No.:

Registration/Matric No.: **KGA130064**

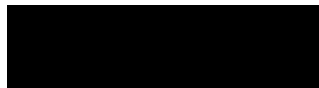Name of Degree: **Masters of Engineering Science**

Title of Project Paper/Dissertation/Thesis: **Behavior of flexural members made from oil palm shell and clinker concrete**

Field of Study: **Civil Engineering (Structure and Materials)**

I do solemnly and sincerely declare that:

(1) I am the sole author/writer of this Work;

(2) This Work is original;

(3) Any use of any work in which copyright exists was done by way of fair dealing and for permitted purposes and any excerpt or extract from, or reference to or reproduction of any copyrighted work has been disclosed expressly and sufficiently and the title of the work and its authorship have been acknowledged in this work;

(4) I do not have any actual knowledge nor do I ought reasonably to know that the making of this work constitutes an infringement of any copyrighted work;

(5) I hereby assign all and every rights in the copyright to this Work to the University of Malaya (UM), who henceforth shall be owner of the copyright in this Work and that any reproduction or use in any form or by any means whatsoever is prohibited without the written consent of UM having been first had and obtained;

(6) I am fully aware that if in the course of making this Work I have infringed any copyright whether intentionally or otherwise, I may be subject to legal action or any other action as may be determined by UM.

Candidate's Signature   Date 10/01/2017

Subscribed and solemnly declared before,

Witness's Signature   Date

Name:

Designation:

ABSTRACT

Waste materials, such as oil palm shell (OPS) and palm oil clinker (POC) from the Malaysian palm oil industry have been used by various researchers to produce lightweight concrete. Concrete containing only OPS showed more ductility and low compressive strength while concrete containing only POC showed less ductility but high compressive strength. The combinations of OPS and POC in concrete seem to be able to improve the compressive strength and ductility behavior. In this study, the possibility of replacing the normal wight aggregate by a mixture of OPS and POC aggregates were investigated. Trial mixes using this mixture of aggregates were carried out to determine the optimum mix ratio. This research also investigated the engineering properties of the concrete mixes and the flexural performance of reinforced palm shell and clinker concrete (PSCC) beams.

Seven PSCC mixes were considered. The proportions of OPS and POC in the concrete mixes were varied from 30% to 70%. In the concrete mix, cement content is kept 450 kg/m^3 which is lowest among the published research so far. The optimum concrete mix was then used in the preparation of the PSCC beams. Eight singly reinforced PSCC beams of dimension 150 mm $\times$ 250 mm $\times$ 3300 with varying reinforcement ratios (0.50 to 2.11%) were prepared. The beams were loaded under four point bending until failure.

The optimum concrete mix obtained from this study achieved compressive strength of about 46 MPa while the ductility index was about 3.56. Other engineering properties such as flexural strength, splitting tensile strength and modulus of elasticity showed good results for structural use. All PSCC beams exhibited typical flexural performance

and experienced ductile failure by giving ample warning before failure. For the beams with higher reinforcement ratio, the deflections at service loads slightly exceeded the values suggested by EC2. The crack widths of PSCC beams satisfied the EC2 requirements for durability aspects. The ultimate moments from the experiment showed slight variations from those predicted by the EC2.

ABSTRAK

Bahan-bahan buangan, seperti sabut dan klinker daripada buah kelapa sawit dalam industri minyak sawit di Malaysia telah digunakan oleh penyelidik untuk menghasilkan konkrit ringan. Konkrit yang mengandungi hanya sabut menunjukkan sifat kemuluran dan kekuatan mampatan yang rendah manakala konkrit yang mengandungi klinker menunjukkan kurang kemuluran tetapi kekuatan mampatan yang tinggi. Gabungan sabut dan klinker dalam konkrit dapat meningkatkan kekuatan mampatan dan sifat kemuluran bahan tersebut. Dalam kajian ini, batuan kasar digantikan dengan campuran sabut dan batuan klinker dalam konkrit untuk mencari nisbah campuran yang optimum. Kajian ini juga mengkaji sifat-sifat mekanikal campuran konkrit dan prestasi lenturan yang diperkukuhkan oleh sabut dan klinker dari kelapa sawit dalam rasuk.

Sejumlah tujuh campuran telah dibuat untuk kedua-dua bahan buangan. Peratusan sabut dan klinker dalam campuran konkrit berbeza dari 30% sehingga 70%. Dalam campuran konkrit, kandungan simen ditetapkan 450 kg/m^3 merupakan yang paling rendah di kalangan kajian yang diterbitkan setakat ini. Selepas itu, campuran optimum diperolehi dan digunakan dalam penyediaan rasuk campuran sabut dan klinker. Sejumlah lapan rasuk bertetulang berdimensi 150 mm $\times$ 250 mm $\times$ 3300 dengan nisbah tetulang yang berbeza-beza (0.50 sehingga 2.11%) disediakan untuk ujian kekuatan konkrit. Rasuk diletakkan di bawah empat lokasi lenturan sehingga gagal.

Campuran optimum yang diperolehi daripada kajian ini mencapai kekuatan mampatan antara 38 sehingga 46 MPa manakala indeks kemuluran antara 3.26 sehingga 3.82. Sifat-sifat mekanikal yang lain seperti kekuatan lenturan, kekuatan tegangan dan modulus keanjalan menunjukkan hasil yang baik untuk kegunaan struktur. Semua rasuk

menunjukkan prestasi lenturan biasa dan kegagalan mulur yang berpotensi dengan memberikan amaran secukupnya sebelum kegagalan. Bagi rasuk dengan nisbah tetulang yang lebih tinggi, pesongan pada beban perkhidmatan melebihi had yang sedikit. Lebar retak rasuk dan keperluan EC2 menunjukkan keputusan yang baik dalam aspek ketahanan. Ramalan menggunakan EC2 menunjukkan keputusan yang baik apabila dibandingkan dengan hasil eksperimen.

ACKNOWLEDGEMENTS

LIST OF CONTENTS

LIST OF FIGURES

LIST OF TABLES

LIST OF NOTATIONS

A_c : Contact area

A_s : Cross-sectional area of steel bar

B : Width of concrete sample

b : Width of the concrete beam specimen

D : Diameter

d : Effective depth of concrete beam specimen

d_c : Depth of concrete cover

E : Modulus of elasticity

E_s : Static modulus of elasticity

$E_{s(pre)}$: Predicted static modulus of elasticity

ε : Strain

ε_c : Strain of concrete

ε_{cu} : Ultimate strain of concrete

ε_s : Strain of main tensile steel

ε_2 : Longitudinal strain due to stress

F_b : Breaking Load

F_c : Concrete crushing Load

F_{cc} : Force carried by the concrete

F_m : Maximum load

F_s : Force carried by the steel bar

f_c : Cube compressive strength of concrete

f_{c1} : 1-day Cube compressive strength of concrete

f_{c3} : 3-day cube compressive strength of concrete

f_{c7} : 7-day cube compressive strength of concrete

f_{c28}	:	28-day cube compressive strength of concrete
f_r	:	Flexural strength of concrete or modulus of rupture
f_t	:	Splitting tensile strength of concrete
f_y	:	Yield strength of steel bar
GPa	:	Giga pascale
H	:	Height of the concrete specimen
h	:	Height of the concrete beam specimen
kN	:	Kilo newton
L	:	Span length
M	:	Moment
M_{des}	:	Theoretical design moment
MPa	:	Mega pascal
M_{ult}	:	Experimental ultimate moment
m	:	Meter
P	:	Ultimate load
ρ	:	Reinforcement ratio
S_1	:	Stress corresponding to a longitudinal strain of 50 millionths
S_2	:	Stress corresponding to a 40% ultimate load
μ	:	Ductility coefficient
V_c	:	Shear capacity of the concrete
V_{cap}	:	Shear capacity of the beam
V_s	:	Shear capacity of the steel bar
w/c	:	Water cement ratio
ω	:	Air-dry density of concrete
x	:	Depth of neutral axis
φ	:	Diameter

σ_{max} :   Peak stress

Δ_{exp} :   Maximum experimental mid span deflection

Δ_{theo} :   Theoretical mid-span deflection

Δ_u :   Experimental deflection at ultimate load

Δ_y :   Experimental deflection at yield load

LIST OF ABBREVIATIONS

ACI   :   American Concrete Institute

ACV   :   Aggregate Crushing Value

AIV   :   Aggregate Impact Value

ASTM   :   American Society for Testing and Materials

BS   :   British Standard

CEB   :   Comité européen du béton

EC2   :   Euro Code 2

ELE   :   Engineering Laboratory Equipment

FIP   :   Fédération Internationale de la Précontrainte

FM   :   Fineness of Modulus

LVDT   :   Linear Variable Displacement Transducer

LWAC   :   Lightweight Aggregate Concrete

LWC   :   Lightweight Concrete

NWC   :   Normal Weight Concrete

OPS   :   Oil Palm Shell

OPKSC :   Oil Palm Kernel Shell Concrete

OPSC   :   Oil Palm Shell Concrete

POC   :   Palm Oil Clinker

POCC   :   Palm Oil Clinker Concrete

PSCC   :   Palm Shell and Clinker Concrete

SP   :   Super Plasticizer

SSD   :   Saturated Surface Dry

UPV   :   Ultra Pulse Velocity

CHAPTER 1: INTRODUCTION

1.1 Background

Lightweight concrete (LWC) is a popular choice in the construction sector. The use of LWC has many advantages over normal weight concrete. Structural lightweight concrete allows engineers to use smaller structural elements due to the reduction of self-weight. The building can be taller using the same foundation and concrete beams can go longer due to the greater span-depth ratio (Chandra and Berntsson, 2002; Shannag, 2000). As a lightweight aggregate concrete (LWAC) reduces the amount of dead load and cost of construction noticeably, it is fair to claim that it has a substantial benefit over normal weight concrete (Lopez et al., 2006). And because of this reason, production of structural lightweight concrete is becoming more popular every day in the construction industry. Lightweight concrete usually has a density of less than 2000 kg/m^3. A lightweight concrete with the compressive strength of more than 17 MPa is recognized as structural lightweight concrete (EC2, 2004).

Lightweight concrete, especially those which are made from lightweight aggregates are most commonly used for the structural purpose and has found many applications in a variety of constructions worldwide such as bridges, precast members, buildings and also offshore structures construction (Chandra and Berntsson, 2002; Raithby and Lydon, 1981). In general, these lightweight concretes produced from expanded clay, shale and pumice are mostly utilized in western countries. However, in developing countries they are not extensively used, which may be due to the limited supply and high production cost of the aggregates.

Malaysia is one of the largest palm oil manufacturing countries in the world. According to Teo et al. (2006c), over 4 (four) million tons of OPS is being produced throughout the country annually as waste materials. However, these OPS were no economic values and were mostly left to decay (Okpala, 1990). In recent years, it is being used as raw burning materials for power production in the palm oil producing factories (Choong, 2012). And the residue from the burning of OPS is known as palm oil clinkers (POC). The shape and size of the OPS and POC are appropriate for considering it as coarse aggregate. At the same time OPS and POC poses the low value of specific gravity which convinces the researchers to use these aggregates to produce lightweight concrete. Moreover, the environmental and economic benefits also made OPS and POC a popular choice as a coarse aggregate in concrete (U. Alengaram et al., 2008; Basri et al., 1999; Mannan and Ganapathy, 2001b; Okpala, 1990; Shafigh et al., 2011b). Concrete which has employed OPS and POC has been termed as oil palm shell concrete (OPSC) and palm oil clinker concrete (POCC) respectively (Ahmmad et al., 2014; Mohammed et al., 2014).

As the research continues on OPSC and POCC, some salient features are discussed in this section. Three singly and three doubly reinforced beams made with OPS concrete were investigated with different reinforcement ratios in the study of Teo et al. (2006b). In their study, the crushing of the compression concrete with sufficient amount of ultimate deflection occurred at the moment of final failure. Yielding of the tensile reinforcement occurred before crushing of concrete at the top of the beam in the pure bending zone. Experimental ultimate moments (M_{ult}) showed good correlation with the theoretical design moments (M_{des}) for all the experimented beams (Teo et al., 2006b). For beams with reinforcement ratio of 3.14% or less, the experimental ultimate moment was about 4 to 35% higher than the expected values. They suggested that for OPS

concrete beams recent code could be used to calculate ultimate moment capacity and deflection for reinforcement ratios up to 3.14%. The flexural performance of reinforced oil palm kernel shell concrete (OPKSC) beams was published by Alengaram et al. (2008) and shows a more ductile behavior than normal weight concrete beams. Mohammed et al. (2014) reported the flexural performance of POC concrete beam considering identical specification as the study of Teo et al. (2006b). They also concluded that even though POCC had a lower value of modulus of elasticity and the deflection of reinforced POCC beams satisfied the BS8110 (1997) under the service load condition.

Several studies have been carried out to aid the understanding of the introduction of OPSC (Alengaram et al., 2011b; Jumaat et al., 2009) and POCC (Ahmmad et al., 2014; Mohammed et al., 2014) concrete mix designs and its material properties. The OPSC or POCC constitutes of cement, sand, OPS or POC and water. It is fascinating that both the OPS and POC have low bulk density. Lightweight concrete can be produced by using OPS and POC as coarse aggregate. Hence, it is of utmost interest to know the behavior of lightweight concrete employing both OPS and POC as coarse aggregate.

1.2 Problem statement

Previous researchers have produced lightweight concrete using OPS with 28-day cube compressive strength of 35 MPa or less (U. Alengaram et al., 2008; Basri et al., 1999; Mannan and Ganapathy, 2001b; Okafor, 1988; Shafigh et al., 2011b). Mannan and Ganapathy (2001a) found the 28-day compressive strength of OPSC in between 20 and 24 MPa depending on the curing conditions by using 480 kg/m^3 cement with w/c ratio of 0.41. The highest 28-days compressive strength was reported by Mannan et al. (2006) which was about 33 MPa with a slump value of 95 mm. Furthermore, the 28-

day compressive strengths of the concrete are in the range of 26 to 36 MPa and slump value was in the range of 0 to 160 mm. They used cement content in the range of 440 to 530 kg/m^3 with 5% fly ash as cement replacement and 10% silica fume as additional cementing material (U. Alengaram et al., 2008). A study has revealed that OPS can be used as a lightweight aggregate for producing high strength lightweight concrete (Shafigh et al., 2011a). In this study OPS aggregate is used as a partial replacement of normal weight aggregate and 28-day compressive strength was found to be in the range of 41 to 43 MPa (Shafigh et al., 2011a).

Existing literature shows that the test results for compressive strength of POC concrete range from 25.5 to 42.56 MPa. It is higher than the minimum required the strength of 17 MPa for structural lightweight concrete (Mohammed et al., 2014). Maximum 28 days compressive strength of POC concrete has been achieved as 44.89 MPa (Ahmmad et al., 2014). The limitation of OPS concrete is that it shows low compressive strength but has a high ductility compared to normal weight concrete (Ahmmad et al., 2014). POC concrete, on the other hand, has a consistent and high compressive strength but has less ductility (Ahmmad et al., 2014). Steel fiber was used to improve the flexural toughness and others mechanical properties Mo et al. (2014b). All the studies employed OPS or POC separately.

From the above discussion, it is clear that both OPS concrete and POC concrete has their advantages and disadvantages. In this study, mix design and the engineering properties of an innovative cleaner and greener concrete containing OPS and POC as a coarse aggregate was investigated. The new concrete made from the local natural waste materials was named as palm shell and clinker concrete (PSCC). The ductility of PSCC

was studied as well. Furthermore, the flexural behavior of reinforced PSCC beam has been investigated.

1.3   Research objective

The main objectives of the study are as follows:

  i.   to find out the mix design that will give the optimum results for making PSCC

  ii.   to determine the engineering properties of PSCC mixes

  iii. to investigate the flexural behavior of reinforced PSCC beams

  iv.   to study the effect of varying reinforcement ratio on the flexural behavior of the PSCC beams.

1.4   Scope of the study

The scopes of this research are presented below:

  i.   this research will be limited to investigating the mix design, workability and density, compressive strength, flexural strength and splitting tensile strength, modulus of elasticity and the stress-strain behavior of PSCC.

  ii.   the stress-strain behavior and ductility properties of PSCC will also be evaluated to assess the suitability in structural elements.

  iii. the flexural study of singly reinforced PSCC beams with varying reinforcement ratio includes the mode of failure, moment capacity, deflection behavior, cracking pattern and steel & concrete strain.

iv. the ductility performance of singly reinforced PSCC beams includes the displacement ductility behavior.

1.5 Organization of thesis

The thesis comprises of five chapters dealing with various aspects of engineering properties of PSCC and the flexural behavior of reinforced PSCC beam. The brief outlines are as follows.

Chapter one gives the overview of the study. At the beginning of the introduction, the background of this research has been described. The basic features and associated advantages of lightweight concrete in construction are summarized. A short discussion of engineering properties of lightweight concrete using OPS and POC agricultural lightweight aggregates is included. Research problem, research objectives and the scope of the study are then discussed. Finally, the chapter ends with the brief thesis layout.

Chapter two is the literature review that begins with a comprehensive literature survey on lightweight concrete. A critical review of the mix design, engineering properties and structural performance of OPSC and POCC is presented in this chapter based on relevant published data. The research gaps are critically identified here to highlight the significance of the newly developed PSCC comprising its structural performance.

Chapter three presents the experimental program of this research to achieve the objectives. The selection and testing of constituent materials are described. The mix design, sample preparation and the testing scheme of PSCC are discussed. Detailed

experimental procedures including beam fabrication and instrumentation for the flexural performance of PSCC beam are also presented in this chapter.

Chapter four describes the detailed experimental results obtained from the research and their critical evaluation in the field of concrete technology using OPS and POC as coarse aggregates to establish a permanent value to the research. The first part of this chapter describes the engineering properties and the ductility performance of PSCC to show the effectiveness of blender of OPS and POC to introduce the salient characteristics of the newly developed lightweight concrete. The second part of the thesis describes the flexural performance of singly reinforced PSCC beam.

Chapter five summarizes with several conclusive remarks based on the major findings of the present research. Moreover, the chapter outlines several important recommendations for further research.

CHAPTER 2: LITERATURE REVIEW

2.1   Introduction

This chapter presents different aspects of lightweight concrete produced from the agricultural waste. The constituent materials used in PSCC and their properties, mix design, are discussed in this chapter. In addition, the major fresh and hardened concrete properties are presented in this chapter. Finally, this chapter identifies a number of research gaps and needs for further study to enhance our understandings.

2.2   Lightweight concrete

The density is the main parameter to define a concrete as lightweight concrete. Usually, lightweight concretes are less dense than the normal weight concretes. According to the application of lightweight concrete, it can be ordered in three categories (Neville, 2008):

i.   structural lightweight concrete (ASTM-C-330-89, 1989): Structural lightweight concrete has a density within the range of 1350 to 2000 kg/m^3 and 28-day compressive strength should be greater than or equal to 17 MPa. This concrete is considered for structural purpose.

ii.   lightweight concrete for masonry units (ASTM-C-331-89, 1989): The usual density of this concrete is between 500 to 800 kg/m^3 and 28-day compressive strength should be in between 7 to 17 MPa.

iii.   low-density or insulation concrete (ASTM-C-332-87, 1989): The usual density of this concrete is between 300 to 800 kg/m^3 and 28-day

compressive strength should be in-between 0.7 to 17 MPa. Furthermore, thermal conductivity coefficient of this concrete should be below 0.3 $J/m^2s^0C/m$.

From the point of view of lightweight concrete's production method, lightweight concrete can be classified into three categories (Neville and Brooks, 2008):

  i. lightweight concrete made from the aggregate which is porous in nature with low specific gravity is known as lightweight aggregate concrete.

  ii. if the air void is introduced in the cement paste to produce the lightweight concrete, this type of lightweight concrete is known as aerated, foam or gas concrete.

  iii. lightweight concrete made by avoiding the fine aggregate between the coarse aggregate particles is widely termed as no-fine concrete.

Lightweight concrete should have the oven-dry density between 300 to 2000 kg/m^3, with 28 day compressive strengths of 1 to over 17 MPa. The coefficient of thermal conductivities of LWC is 0.2 to 1.0 W/mk (Newman and Owens, 2003). The properties of structural lightweight concrete are very similar to other lightweight concrete except higher 28 days compressive strength. According to Shannag (2011), the typical density of structural lightweight concrete ranges from 1400 to 2000 kg/m3 and Kosmatka et al. (2002) suggested that the typical compressive strength range should be from 20 to 35 MPa. Various pozzolans such as fly ash, silica fume, metakaolin, calcined clays and shales can be used to produce high strength (35 to 70 MPa) lightweight aggregate

concrete with a maximum w/c ratio of 0.45 (Holm and Bremner, 2000). Generally, the compressive strength enhancement can be achieved by reducing the coarse aggregate size and or partially substituting the lightweight fine aggregate by a good quality normal weight sand at a given cement and water content (Mehta and Monteiro, 2006).

2.3   OPS and POC as lightweight aggregate

Malaysia is the second largest source of palm oil in the world (Teo et al., 2006c). Palm factories in Malaysia produces a huge quantity of solid waste. The residue of palm oil industries includes OPS and POC (Figure 2.1 and Figure 2.2). Recently these waste materials are being used in land filling and production of charcoal. It causes not only soil pollution but also affects the groundwater supply source. Therefore, using them as a building construction material is turning waste into resources leading to a very efficient waste management option as well as a very useful structural design option. It will sustain the ecological balance and preserve natural resources.

Figure 2.1: Mass storage of oil palm shell (OPS) (Teo et al., 2006c)

The production of LWC using OPS as a lightweight aggregate was started in early 1985 (Salam et al., 1985). Further research revealed that POC can also be used along with OPS as a lightweight aggregate to produce the structural lightweight concrete. (Abdullah, 1996; Basri et al., 1999; Mannan and Ganapathy, 2001b; Teo et al., 2007).

Figure 2.2: Storage of palm oil clinker (POC)

2.4   Properties of OPS aggregate

Palm oil production from raw palm fruits goes through six successive process: sterilization, threshing, pressing, depericarping, separation of palm kernel and palm shell, and clarification (Abdullah, 1996). Oil palm shell is one of the byproducts of this process. The color for oil palm shells is dark gray to black.

2.4.1 Shape, thickness, texture

The oil palm shells are found in different shapes depending on the breaking pattern of the nut. The OPS has concave and convex faces. The surfaces of the concave and convex faces are fairly smooth and the broken edges are spiky. The thickness of the OPS varies depending on the type of palm tree from which the nuts are obtained. Generally, it ranges between 0.15 to 8 mm (Basri et al., 1999; Okpala, 1990). It is worth mentioning that Shafigh et al. (2011a) have reported that OPS aggregate produced from crushing the larger original OPS aggregate can be used in enhancing the compressive strength of lightweight OPS concrete. According to their study, after collection of OPS, it has been washed and crushed by using a stone-crushing machine in the laboratory to get the desired size of aggregate. Figure 2.3 shows a process flow of OPS aggregate. The chemical composition of OPS aggregates shown in Table 2.1.

Table 2.1: Chemical composition of OPS aggregate (Teo et al., 2007)

Elements	Results (%)
Ash	1.53
Nitrogen (as N)	0.41
Sulphur (as S)	0.000783
Calcium (as CaO)	0.0765
Magnesium (as MgO)	0.0352
Sodium (as Na_2O)	0.00156
Potassium (as K_2O)	0.00042
Aluminum (as Al_2O_3)	0.130
Iron (as Fe_2O_3)	0.0333
Silica (as SiO_2)	0.0146
Chloride ((as Cl-)	0.00072
Loss on Ignition	98.5

2.4.2 Water absorption

The 24-hour water absorption capacity of OPS is in the range of 21 to 33%. That means OPS has a higher level of water absorption capacity compared to the normal weight

aggregates (less than 2%) (Neville, 2008). This high water absorption is made possible by 37% porosity of the shell (Okpala, 1990). OPS can absorb more water than relatively nonporous materials like gravel, as it is highly porous material. Mannan et al. (2006) reported that a pre-treatment by 20% polyvinyl alcohol solution can drop the water absorption of OPS significantly from 23.3% to 4.2%, thus improve the quality of OPS.

Figure 2.3: OPS aggregates: (a) original size, (b) original small size and (c) crushed from original size (Shafigh et al., 2011a)

2.4.3 Bulk density and specific gravity

Due to the higher porosity of OPS than normal weight aggregates, loose and compacted bulk densities varies in the range of 500 to 600 kg/m^3 and 590 to 620 kg/m^3; respectively. The specific gravity of OPS varies in between 1.14 to 1.37. The densities of OPS are nearly 60% lighter than normal weight coarse aggregates. Thus, it falls in the range of light weight aggregate and concrete using OPS aggregate exhibits lightweight concrete (Okafor, 1988; Okpala, 1990).

2.4.4   Compressive and impact value

Experimental results show that the OPS is hard and naturally it does not erode easily. Basri et al. (1999) reported that the Los Angeles abrasion value of the OPS and crushed stone is 4.8% and 24%, respectively. These values indicate that OPS aggregates have stronger resistance to wear than conventional coarse aggregates. Furthermore, OPS aggregates show better shock absorbing qualities as the properties like aggregate impact value and crushing value is lower than that of conventional aggregates (Teo et al., 2007). The indirect compressive strength of the OPS aggregate is 12.1 MPa with 2 MPa standard deviation (Okpala, 1990). Overall these shells are subjected to withstand variable braking forces. Particles of these shells can be very useful in brake lining formulations with other additives (Koya and Fono, 2009).

2.5   Properties of POC aggregate

Malaysian palm oil industries burn the palm oil waste to yield steam needed for the milling process. Palm oil clinker (POC) is produced as a by-product of burning process (Mohammed et al., 2011). Their color ranges from gray to black. After processing this raw POC, it is being used to produce lightweight concrete. A process flow of POC aggregate is shown in Figure 2.4.

Figure 2.4: A process flow of POC aggregate (Mohammed et al., 2014)

2.5.1 Shape and texture

The raw POC was collected from the palm oil processing mill. After crushing and sieving of raw POC, expected particle sizes of aggregates are achieved (Mohammed et al., 2013). The POC aggregates can be found in different shape like angular, polygonal etc., subjected to the breaking pattern of the raw POC. The faces of the POC are very rough and porous. However, the broken edge is spiky. Usually, fine aggregates have the particles size less than 5 mm and particles size between 5 to 14 mm are considered as coarse aggregates. The pore space of the POC coarse aggregate will be occupied by the fine aggregate along with cement paste. On the other hand, the pore spaces of the fine aggregate will be packed by cement paste creating a strong matrix in concrete. Table 2.2 shows the chemical composition of POC aggregate.

Table 2.2: Chemical composition of POC aggregate (Ahmmad et al., 2014)

Elements	Results (%)
Silica (as SiO_2)	59.63
Potassium (as K_2O)	11.66
Calcium (as CaO)	8.16
Phosphorus (as P_2O_5)	5.37
Magnesium (as MgO)	5.01
Iron (as Fe_2O_3)	4.62
Aluminum (as Al_2O_3)	3.7
Sulfur (as SO_3)	0.73
Sodium (as Na_2O)	0.32
Titanium (as TiO_2)	0.22
Others	0.58

2.5.2 Water absorption

The 24-hour water absorption capacity of POC is 4.35%. This value indicates that the POC has a higher level of water absorption capacity compared to the normal weight aggregates which usually have the water absorption capacity below 2% (Neville, 2008). In general, lightweight aggregate has higher water absorption values compared to normal weight aggregate. Among the lightweight aggregates, POC has lower water absorption capacity as indicated by the water absorption values. Higher water absorption was stated for OPS and pumice aggregate of about 37% (Hossain, 2004). Lightweight aggregate concrete has an internal water supply stored in the porous lightweight aggregate. Due to this water, lightweight concrete is less sensitive to the poor concrete at their early ages compared to the normal weight concrete (Al-Khaiat and Haque, 1998).

2.5.3 Bulk density and specific gravity

POC aggregates are porous in nature. Therefore, low bulk density and high water absorption were expected. The specific gravity of POC varies in the range of 1.7 to 1.82. POC coarse aggregate has a unit weight of 781 kg/m^3 which is around 48% lighter than the crushed granite stone (Teo et al., 2006c). Thus, it falls in the range of light weight aggregate and concrete using POC aggregate exhibits lightweight concrete (Okafor, 1988; Okpala, 1990).

2.5.4 Compressive and impact value

Higher aggregate impact value (AIV) and aggregate crushing value (ACV) of POC aggregates have been reported 34% and 30% higher than the normal weight aggregates respectively (Teo et al., 2006b). The higher ACV value for the POC aggregate might be caused by the particle shape of the used POC in that study which is permeable and

slanted. This specific shape and spongy condition made POC more vulnerable to get crushed under load.

2.6   Concrete with OPS aggregate

2.6.1   Mix design

For a particular compressive strength, cement content is fairly constant in well-proportioned concrete mixtures. Hence, several trial mixtures are required with varying cement contents in producing a range of compressive strengths (Kosmatka et al., 2002). The oil palm shells tend to segregate in wet concrete mixes due to its lighter weight in the cement matrix. A good mix design can only be found through the trial mixes (Abdullah, 1996). Mix design methods for normal weight concrete are not compatible with the lightweight aggregate concrete (Mannan and Ganapathy, 2001b; Shetty, 2005). In a large experimental set, they used lightweight aggregate such as; Leca, fumed slag, Aglite and Lytag in mixed design method. However, same methods were found not suitable for OPS concrete. As a reason for such behavior of OPS, they pointed out the natural organic property of OPS with a smooth texture and varying shapes. Table 2.3 summarizes the mix designs of OPS concrete used for the investigation of reinforced OPS concrete beam in previous studies. This guideline can be used for future investigations since the resulting reinforced concrete beams performed satisfactorily.

Table 2.3: Acceptable mix proportion of OPS concrete (Mo et al., 2014a)

Mix design of OPS concrete	Mix proportion Cement : sand : LWA : water	Remarks
Teo et al. (2006b) Teo et al. (2006c) Teo et al. (2006a)	1 : 1.66 : 0.60 : 0.38	Cement content fixed at 510 kg/m^3
Alengaram et al. (2008)	1 : 1.20 : 0.80 : 0.40	Cement content fixed at 480 kg/m^3 5% fly ash added 10% silica fume added 1.0% superplasticizer added
Alengaram et al. (2011a)	1 : 1.20 : 0.80 : 0.40	Cement content fixed at 500 kg/m^3 5% fly ash added 10% silica fume added 1.0% superplasticizer added
Jumaat et al. (2009)	1 : 1.20 : 0.80 : 0.40	Cement content fixed at 420 kg/m^3 6.7 kg/m^3 foam content used 5% fly ash added 10% silica fume added 0.5% superplasticizer added
Ahmed and Sobuz (2011)	1 : 1.71 : 0.39 : 0.41 1 : 1.65 : 0.25 : 0.45 1 : 1.65 : 0.37 : 0.45	50% OPS + 50% granite 10% OPS + 90% granite 15% OPS + 85% granite
Muda et al. (2012)	1 : 1.5 : 0.45 : 0.40	5% silica fume added 2.0% superplasticizer added

2.6.2 Slump

To check the uniformity of concrete mix based on the given proportions, Slump test is very useful (Neville, 1995). It is the standard test to understand the workability of concrete. It measures the consistency of concrete according. The slump value of concrete rises with the water-cement ratio. The slump value of OPS concrete to be found very low (0 to 4 mm) indicating a very low workability (Mannan and Ganapathy, 2001b; Neville, 1995; Okafor, 1988; Okpala, 1990). At the earlier age of research on OPS, Abdullah (1996) achieved 15MPa compressive strength with slump values in the range of 0 to 260 mm. High slump value (105 mm) is achievable by adding a minute percentage of superplasticizer (Alengaram et al., 2010).

2.6.3 Density

The density is the most important factor for the structural applications of lightweight concrete (Rossignolo et al., 2003). The typical density of lightweight concrete is between 1400 to 2000 kg/m^3. Whereas normal weight concrete has the density of 2400 kg/m^3 (Chen and Liu, 2005). Okafor (1988) reported the possibility of concrete production with a density of approximately 1758 kg/m^3 using agricultural solid waste like OPS. According to Basri et al. (1999), OPS concrete has 19 to 20% lower air-dry densities than normal weight concrete. Other studies show that OPS concrete is 22% (Mannan and Ganapathy, 2004) and 24% (U. Alengaram et al., 2008) lower in density than the normal weight concrete. Furthermore, it was reported that OPS concrete having 10% and 15% fly ash are 2% and 3% lower than OPS concrete without fly ash content (Mannan and Ganapathy, 2004).

2.6.4 Compressive strength

To define the excellence of concrete in practice, the most commonly used parameter is the compressive strength (Wiegrink et al., 1996). Neville and Brooks (2008) suggested a minimum 28-day compressive strength of 17MPa for structural purpose. As per ACI Committee 211.2 (1998), the projected relationship between average compressive strength and cement content of structural lightweight concrete is shown in Table 2.4.

Table 2.4: Approximate relationships between average compressive strength and cement content of structural lightweight concrete (ACI Committee 211.2, 1998)

Compressive strength (MPa)	Cement content (kg/m^3)	
	All-lightweight	Sanded-lightweight
17	240-305	240-305
21	260-335	250-335
28	320-395	290-395
34	375-450	360-450
41	440-500	420-500

The typical compressive strength for structural lightweight concrete is 20 to 35 MPa (Kosmatka et al., 2002). Whereas, for the OPS aggregates, the compressive strength is between 25 to 35 MPa (Okafor, 1988). Experiments reported in literature showed different compressive strengths of LWC produced from OPS aggregates. Mannan and Ganapathy (2001b) found compressive strengths of 20 and 24 MPa when mixing 480 kg/m^3 cement at w/c ratio of 0.41 and mix proportion of 1: 1.71: 0.77 by weight of cement, sand and OPS aggregate. U. Alengaram et al. (2008) achieved the maximum compressive strength of 36 MPa by using fly ash and silica fume, a sand to cement ratio of 1.6, and water to binder ratio of 0.35. Okafor (1991) tested a superplasticizer in Palm Kern Shell (PKS) concrete. With the increase of superplasticizer from 0 to 2.5%, the compressive strength of PKS lightweight concrete for water to cement ratios of 0.45 and 0.50 rises. Higher dispersion of cement particles enables this strength. However, at the higher water to cement ratio of 0.60 and level of dosage of 2.5%, the compressive strength drops in all corresponding mix with an admixture dosage of 2%. This is due to bleeding and segregation in the concrete.

Mannan et al. (2006) improved in quality of OPS aggregates significantly by giving 20% polyvinyl alcohol as a pretreatment to OPS. These pre-treated OPS showed an increase in compressive strength 35.3%, 38.8% and 39.2% at 3, 7 and 28 days, respectively. He also reduced the water absorption of this aggregate from 23.3% to 4.2% and achieving superior adhesion between the OPS and cement paste. This improved the compressive strength.

Basri et al. (1999) found the compressive strength of OPS concrete about half of ordinary concrete. On the basis of Okafor's investigation (Okafor, 1988), OPS performs

satisfactorily as a lightweight concrete in middle and low strength concrete. A recent study at the University of Malaya has found applicability of OPS as a lightweight aggregate for producing high strength lightweight concrete (Shafigh et al., 2011a). In their study normal weight aggregate is used as a partial replacement of OPS aggregate and 28-day compressive strength has been found in the range of 41 to 43 MPa.

2.6.5 Splitting tensile strength

In designing of the structural element, the compressive strength is deemed as the most important property of concrete. Additionally, the shear strength, resistance to cracking; the tensile strength is also considered for special structures like a highway, airfield slabs (Neville, 2008). A maximum splitting tensile strength of 2.0 MPa is a prerequisite for structural lightweight aggregate concrete (Holm and Bremner, 2000). Several studies (Abdullah, 1996; U. Alengaram et al., 2008; Mannan and Ganapathy, 2002; Teo et al., 2006c) showed that the splitting tensile strength of continuous water cured OPS concrete at 28-day varied from about 1.1 to 2.4 MPa. This is about 6 to 10% of the corresponding cube compressive strength. For cold-bonded fly ash aggregates, this percentage is about 8 to 10% with the compressive strength ranging from 21 to 47 MPa (Gesoğlu et al., 2004). The ratio of splitting tensile strength to a corresponding compressive strength of about 21 to 24%. It was reported for crushed basaltic-pumice lightweight concrete with a 28-days compressive strength between 28 to 38.9 MPa (Kılıç et al., 2003). In most cases, the splitting tensile strength of lightweight concrete for cube compressive strengths of 20, 30, 40 and 50 MPa is in the range of 1.4 to 2, 1.8 to 2.7, 2.2 to 3.3 and 2.5 to 3.8 MPa, respectively (CEB/FIP, 1977).

The tensile strength of the concrete is related to shear resistance, torsion, anchorage and bond strength, and crack resistance, which can be calculated from its relationship with

compressive strength. (Mahmud, 2010) presented expressions for OPS concrete by the Equation 2.1 and Equation 2.2

$$f_t = 0.57 \sqrt{f_c} - 1.17 \ (R^2 = 0.88) \tag{2.1}$$

Or

$$f_t = 0.20 \sqrt[3]{f_c} \ (R^2 = 0.84) \tag{2.2}$$

where, f_t is the splitting strength and f_c is the compressive strength of cubes, both in MPa.

For cold-bonded fly ash lightweight aggregates concrete, there is a relation between splitting tensile and cube compressive strength for compressive strength ranging from 20.8 to 47.3 MPa, as given in Equation 2.3 (Gesoğlu et al., 2004)

$$f_t = 0.27 \sqrt[3]{f_c^2} \tag{2.3}$$

The relation reported by Neville (2008) is given in Equation 2.4 for pelletized blast furnace slag lightweight aggregate concrete for a compressive strength of between 10 and 65 MPa:

$$f_t = 0.23 \sqrt[3]{f_c^2} \tag{2.4}$$

The tensile strength of structural lightweight concrete is less than the tensile strength of the similar grade normal weight concrete because lightweight aggregate has a lower stiffness than normal weight aggregate (Al-Khaiat and Haque, 1998). Mannan and Ganapathy (2002) found the tensile strength for OPS concrete as nearly 10% of the 28-day compressive strength. They also concluded that the behavior of OPS concrete in this respect is very similar to that of normal weight concrete.

2.6.6 Flexural tensile strength

The curing method greatly influences the flexural tensile strength of LWC than the normal weight concrete (CEB/FIP, 1977). The dried flexural members showed extreme sensitivity to moisture (Mehta and Monteiro, 2006). For continuously moist cured concrete, the flexural strength of lightweight aggregate concrete is 9 to 11 percent of the compressive strength but in air-drying regimes, the flexural strength is normally less than 4% of the compressive strength. Furthermore, in this regime flexural strength is 60% to 70% of the splitting tensile strength. But when moist cured, the flexural strength is usually 50% greater than the splitting tensile strength (Holm and Bremner, 2000).

Lo et al. (2004a) compared to the lightweight concrete based on expanded clay lightweight aggregates to the OPS concrete. The best fit equations for the flexural tensile strength (f_r) of OPS concrete are calculated based on Equation 2.5 and Equation 2.6 (Mahmud, 2010)

$$f_r = 0.58 \sqrt{f_c} \ (R^2 = 0.84) \tag{2.5}$$

Or

$$f_r = 0.33 \sqrt[3]{f_c} \ (R^2 = 0.87) \tag{2.6}$$

where, f_r is flexural tensile strength and f_c is cube compressive strength in MPa.

Lo et al. (2004a) proposed the relationship between the flexural and cube compressive strength of expanded clay aggregate concrete at 28-days can be represented as Equation 2.7. Using this equation, it was determined that their measured flexural strength is marginally lower than the past research findings for concrete mixes of similar compressive strength.

$$f_r = 0.69 \sqrt{f_c} \tag{2.7}$$

For cube strengths ranging from 20 to 60 MPa, another relationship between the compressive strength and the flexural tensile strength of moist cured, lightweight concrete was made using expanded shale and clay aggregates. This is provided by Equation 2.8 (CEB/FIP, 1977):

$$f_r = 0.46 \sqrt[3]{f_c^2} \tag{2.8}$$

This shows that, in general, the flexural strength of OPS lightweight concrete is lower than the lightweight concrete made with artificial lightweight aggregates.

2.6.7 Modulus of elasticity (E)

The most important engineering properties of concrete in designing of structural elements is the modulus of elasticity (Young's modulus). In the prediction of the deformation of reinforced concrete structures, modulus of elasticity is a key influencing factor. The modulus of elasticity of concrete is governed by the moduli of elasticity of its components. It depends on the modulus of elasticity of the matrix, type of aggregates, the effective water-to binder ratio, and the volume of the cement (Chandra and Berntsson, 2002).

The modulus of elasticity of OPS concrete is in the range of about 5 to 11 GPa for a compressive strength range of 24 to 37 MPa (Alengaram et al., 2008; Mannan and Ganapathy, 2002; Teo et al., 2006b; Teo et al., 2006c). For similar strength, the modulus of elasticity of lightweight aggregate concretes is 25 to 50% lower than normal weight concrete (Neville and Brooks, 2008). The elastic modulus of normal weight concrete is higher because the modulus of the normal weight aggregate particles is greater than the modulus of the lightweight aggregate particles (Holm and Bremner, 2000). For example, the modulus of elasticity of expanded clay and shale aggregates is between 5 to 15 GPa, however, this value for dense natural aggregates such as quartz,

limestone and basalt is about 60, 80 and 100 GPa, respectively (CEB/FIP, 1977). Wilson and Malhotra (1988) reported that the modulus of elasticity of lightweight concrete made with expanded shale lightweight aggregate ranges from 23.8 to 27 GPa, for compressive strength range of 33.6-60.8 MPa. (Rossignolo et al., 2003) reported that at the age of 7-days the modulus of elasticity and compressive strength of the Brazilian lightweight aggregate (expanded clay) concrete varied from 12 to 15.2 GPa and 39.7 to 51.9 MPa, respectively. The modulus of elasticity of structural lightweight concrete ranges between 10 and 24 GPa, which is generally much less than that of normal aggregate concrete (CEB/FIP, 1977). The lower modulus of elasticity of lightweight aggregate concrete allows the development of a higher ultimate strain, compared with normal weight concrete of the same strength (Neville, 2008).

Therefore, researchers suggested some unique formulas to predict the modulus of elasticity for light weight concrete. Equation 2.9 was mentioned in CEP/FIP manual (Short and Kinniburgh, 1978). Equation 2.10 and Equation 2.11 was suggested for the OPS concrete (Ahmmad et al., 2014; Alengaram et al., 2011b).

$$E_{s(pre)} = [\omega/2400]^2 x f_c^{1/3} x 9.1 \qquad (2.9)$$

$$E_{s(pre)} = [\omega/2400]^2 x f_c^{1/3} x 5.0 \qquad (2.10)$$

$$E_{s(pre)} = 0.0005 x f_c^{2.69} \qquad (2.11)$$

where, $E_{s(pre)}$ (GPa) is the predicted elastic modulus, f_c (MPa) is cube compressive strength and ω (kg/m^3) is the air dry density of concrete.

These values show that the modulus of elasticity of OPS lightweight concrete is among the lowest of normal weight concrete and significantly lower than other types of lightweight aggregate concrete. To protect slabs and beams from this possible excessive deformation due to this low elasticity modulus, the span lengths should be kept as

small as possible and slab depths are kept a little greater than customary values. The example given by Sylva et al. (2004) shows that lower E in LWC compared to NWC and, hence higher pre-stress loss in LWC. A girder designed with lightweight concrete would require approximately 8 additional strands to maintain the same effective pre-stress force as a normal weight girder. A previous study by Teo et al. (2006b) showed that the deflection of a beam made with OPS concrete (cube compressive strength of 26.3 MPa and modulus of elasticity of 5.28 GPa) with a reinforcement ratio of 1.13% exceeded the maximum value as provided by BS8110 (1997). They recommended larger beam cross-sections for higher load capacity by OPS concrete.

2.6.8 Flexural behavior of OPSC beams

Teo et al. (2006b) and Alengaram et al. (2008) studied the flexural behavior of reinforced beams. Figure 2.5 shows the failure modes of OPS concrete beam. Various reinforcement ratios were utilized to test six beams, which included both singly and doubly reinforced beams (Teo et al., 2006b). The constant moment region was noticed to produce perpendicular flexural cracks. Thus because of the breakdown of the compression concrete with sufficient ultimate deflection, the final failure was caused due to the crushing of the compression concrete with a significant amount of ultimate deflection. As the entire set of beams was under-reinforced, the tensile reinforcement reached the yield point prior to the crushing of the concrete covering in the pure bending region. Ultimately the concrete cover crushed at the time of the failure causing major deflection. When the experimental ultimate moments (M_{ult}) and the theoretical design moments were compared, the results pointed out a nearer relationship in case of doubly reinforced beams as compared to singly reinforced ones (Teo et al., 2006b). The theoretical design moment (M_{des}) of the beams was anticipated by applying the rectangular stress block analysis which was suggested by BS8110 (1997). When the

reinforcement ratio of the beam is 3.14% or less, the experimental ultimate moment was about 4 to 35% greater than the anticipated values. It was derived that in the case of OPKSC beams, BS8110 (1997) can be utilized to get a conservative estimation of the ultimate moment capacity and sufficient load factor against failure for reinforcement ratios up to 3.14%. The beam possessing the maximum reinforcement ratio of 3.14% induced a bit larger mid-span deflection as compared to the other two beams which demonstrate more ductile characteristics. The ductile characteristics and moment-curvature for OPKSC beams followed similar tendency like the NWC beams (Teo et al., 2006b).

Figure 2.5: Failure modes of OPS concrete beam (Alengaram et al., 2008)

2.7   Concrete with POC aggregate

2.7.1   Mix design

The mix proportioning can be carried out with trial mixes or according to the requirements of ACI Committee 211.2 (1998) or as stated in the prerequisites of the BS code. There is some evidence for mix design of POCC can be found from the previous research work (Kanadasan and Razak, 2014). Omar and Mohamed (2002) used the mix proportion of cement, sand and LWA as 1: 0.95: 1.26. The water-cement ratio was 0.40.   They used 500 kg/m^3 cement content with this mix proportion to get the

lightweight concrete having the compressive strength of 35 MPa. Mohammed et al. (2013) carried out a study including water–cement ratio of 0.40 to 0.46 and cement content of 480 to 520 kg/m^3 according to ACI Committee 211.2 (1998). The test outcomes in case of compressive strength extend from 25.5 to 42.56 N/mm^2.

Five mixing proportions were taken to justify the engineering properties of POCC. In their study, the coarse aggregates were taken in a dry condition as POC drops moisture easily to the air. Because of high water absorption of POC, the aggregates were pre-soaked for 24 hours in water prior to mixing. Hence, saturated surface dry (SSD) state of POC aggregate was attained. This is expected to prevent further absorption during mixing. For letting the cement paste to cover the aggregate allowing the absorbed water to be reserved and for inhibiting the retention of water or penetration of cement paste into the aggregate, two-step mixing procedure was applied. Table 2.5 summarizes the mix designs of POC concrete used for the investigation of reinforced POCC beam in the previous study. This guideline can be used for future investigations since the resulting reinforced concrete beams satisfactorily performed.

Table 2.5: Acceptable mix proportion of POC concrete (Mo et al., 2014a)

Mix design	Mix proportion Cement : sand : LWA	Water cement ratio
Omar and Mohamed (2002)	1 : 0.95 : 1.26	0.40
Mohammed et al. (2011) Hussein et al. (2012)	1 : 1.48 : 0.69	0.44
Mohammed et al. (2013)	1 : 0.95 : 0.31 1 : 0.95 : 0.31 1 : 0.95 : 0.31	0.20 0.40 0.60

2.7.2 Slump

It is found that the slump value of POC concrete goes up along with the water cement ratio alike the normal concrete. Hilton et al. (2007) achieved 105 to 125 mm slump by

using 0.55 w/c ratio. Mannan and Neglo (2010) attained 40 to 70 mm slump by using 0.48 to 0.57 w/c including a small percentage of superplasticizer (SP). Ahmmad et al. (2014) found 124 mm slump with 0.33 w/c adding 1.6% superplasticizer. High range water reducing admixtures can disperse cement grains which result a high slump value contributing a good workability.

2.7.3   Density

There are studies to evaluate the density of POC concrete according to the requirement of lightweight concrete (Chen and Liu, 2005). Hilton et al. (2007) found the density of saturated surface dry condition falls within the limit of the ranges of lightweight concrete. In their study, series using the only POC as coarse aggregates and natural sand offered the density around 2000 kg/m^3 and series using POC as coarse and fine aggregates presented the density around 1850 kg/m^3. These values are 19% and 26% lower than the normal weight concrete respectively. Mannan and Neglo (2010) reported the concrete with POC aggregate exhibiting the mean density below 2000 kg/m^3. Mohammed et al. (2011) got the density of POC concrete about 1769 kg/m^3. From the above discussion, it can be concluded that the concrete from the POC aggregates produces lighter structures.

2.7.4   Compressive strength

As the compressive strength is the most important to describe the excellence of concrete, the projected relationship between average compressive strength and cement content of structural lightweight concrete is shown in Table 2.4.

Mohammed et al. (2011) have exposed that the maximum compressive strength of lightweight concrete produced using this POC is approximately 30.9 MPa. This is

within the typical compressive strength for structural lightweight concrete of 20-35 MPa (Kosmatka et al., 2002). Mohammed et al. (2013) exhibited that by using 480 kg/m^3 cement, a free water to cement ratio of 0.40 and POC aggregate, the 28-day compressive strength of OPS concrete is between 25.5 to 42.56 MPa. Hilton et al. (2007) found the 28-day compressive strength, of about 33.7 MPa which was achieved by using 420 kg/m^3 cement and water to cement ratio of 0.35. They also tried to use the fly ash with cement to produce lightweight concrete. They used 90% cement and 10% fly ash. Ahmmad et al. (2014) used 482 kg/m^3 cement content with W/C 0.33 to produce LWC. The compressive strength of POC lightweight concrete was 44.89 MPa. So far this strength was the maximum. Therefore, it can be concluded that with cement content of 450 to 480 kg/m^3 and a water to cement ratio of 0.32 to 0.42, the 28-days compressive strength can be found 35 to 45 MPa

2.7.5   Splitting tensile strength

Splitting tensile strength of concrete is a very important parameter to calculate the cracking behaviors. Previous studies linked their finding to the existing code and practice to show the effectiveness of POC concrete (Holm and Bremner, 2000). Several studies (Hilton et al., 2007; Mohammed et al., 2011; Mohammed et al., 2013) show that the splitting tensile strength of continuous water cured POC concrete at 28-day varied from about 2.1 to 4.2 MPa. This is about 6 to 12% of the corresponding cube compressive strength. In general, the splitting tensile strength of lightweight concrete for cube compressive strengths of 20, 30, 40 and 50 MPa is in the range of 1.4 to 2, 1.8 to 2.7, 2.2 to 3.3 and 2.5 to 3.8 MPa, respectively (CEB/FIP, 1977).

2.7.6 Flexural tensile strength

The flexural tensile strength of POC concrete stated by various researchers. Mohammed et al. (2011) and Mohammed et al., (2014) performed an experimental investigation using POC aggregates. As POC aggregate has many pores, they attained the flexural tensile strength in the range of 3.5 to 4.6 MPa and it was approximately 10% of the compressive strength of POC concrete. Zakaria (1986) also conducted an experimental investigation using normal weight sand and POC as coarse aggregates. He achieved the flexural tensile strength in the range of 3.0 and 5.0 MPa and it was approximately 20% of the compressive strength of concrete.

2.7.7 Modulus of elasticity (E)

The modulus of elasticity of POC concrete is in the range of about 16 to 22 GPa for a compressive strength range of 31 to 44 MPa (Ahmmad et al., 2014; Mohammed et al., 2011). For the similar grade compressive strength, the modulus of elasticity of lightweight aggregate concretes is 6 to 20% lower than normal weight concrete (Neville and Brooks, 2008). Wilson and Malhotra (1988) reported that the modulus of elasticity of lightweight concrete made with expanded shale lightweight aggregate ranges from 23.8 to 27 GPa, for compressive strength range of 33.6 to 60.8 MPa. Rossignolo et al. (2003) reported that at the age of 7 days the modulus of elasticity and compressive strength of the Brazilian lightweight aggregate (expanded clay) concrete varied from 12 to 15.2 GPa and 39.7 to 51.9 MPa, respectively. The modulus of elasticity of structural lightweight concrete ranges between 10 and 24 GPa, which is generally much less than that of normal aggregate concrete (CEB/FIP, 1977). Values show that modulus of elasticity of POCC is much better than the OPSC.

2.7.8 Flexural behavior of POCC beams

Mohammed et al. (2014) investigated the effect of varying tension reinforcement ratios of the reinforced POC beams, ranging from 0.35% to 2.23%. All the reinforced POC beams exhibited typical flexural failure, which suggested the use of POC did not bring upon the detrimental effect on the flexural behavior of reinforced concrete beam. The experimental value of the moment capacity of the reinforced POC beams was close to the prediction using BS 8110 design method, as only 1 to 7% difference. However, the experimental serviceability deflection values were about 10 to 45% lower compared to BS 8110. Despite this, the serviceability deflection for the singly reinforced POC beams was acceptable since it adhered to the limit stated in BS 8110. In the case of the doubly reinforced POC beams, similar to the finding by Teo et al. (2006b), it was recommended that larger beam depths should be used to ensure a satisfactory span-deflection ratio. Apart from that, it was found that ACI 318 and BS 8110 gave reasonable crack width prediction at service loads for the reinforced POC beams. In addition, the crack widths at service loads obtained from the study were below the maximum permissible limit stipulated in ACI 318 and BS 8110. Figure 2.6 shows the Crack patterns and failure mode of POC concrete beam.

Based on the research carried out by Mohammed et al. (2014), it could be summarized that the use of POC in reinforced concrete beam was suitable for structural application since most of the behavior conformed to design codes and also comparable to other types of reinforced LWC beams done previously. Mohammed et al. (2013) also investigated the shear behavior of reinforced POC beams with varying tension reinforcement ratios, shear span to effective depth ratio, and compressive strength of POC. In general, the shear failure cracking observed for the reinforced POC beams was similar to that of conventional reinforced NWC beams. The increase in tension

reinforcement ratio and compressive strength led to the increase in the shear strength of the reinforced POC beams while the effect of shear span to effective depth ratio on the reinforced POC beams was similar to that for conventional reinforced NWC beams. It is noteworthy that the shear strength prediction based on BS 8110, ACI, and EC2 overestimated the shear capacity of the reinforced POC beams and safety precaution should be taken to avoid the shear failure of reinforced POC beam. The reinforced POC beam showed similar shear failure as what would be expected of conventional reinforced concrete beam and this further justifies the usage of POC in reinforced concrete beam, bearing in mind that adequate safety factor should be applied when considering the ultimate shear capacity.

Figure 2.6: Crack patterns and failure mode of POC concrete beam (Mohammed et al., 2014)

2.8   Research gaps

From the literature review carried out, number of research gap could be identified. The most critical which formed the basis of this study are as follows:

i.   Both OPS concrete and POC concrete have their own advantages and disadvantages. It seemed that no research work in combining OPS and POC aggregate to produce high strength lightweight concrete has been reported.

ii. From the literature review, the behavior of structural members made from PSCC has not been studied yet.

iii. The current design procedures by EC2 for flexural strength of both the lightweight aggregate concrete and the normal weight concrete are derived from the understanding of concrete made with normal aggregates. Hence, it is apparent that the current design procedures by EC2 may not be suitable to predict the ultimate flexural resistance of the PSCC beams. Since no guidance has been given in EC2, therefore, it is essential to carry out an investigation to aid the current understanding of flexural strength of the PSCC beams.

CHAPTER 3: METHODOLOGY

3.1   Introduction

This chapter discusses the overall research procedures used for this study. The experimental investigation involved in this research is described in this chapter. The selection and testing materials, the preparation of aggregates, the mix design of concrete, and the preparation of beams are presented in this chapter. In addition, testing processes employed in the investigation of the fresh and hardened concrete properties and flexural performance of reinforced PSCC beams are discussed in this chapter.

3.2   Research procedure

This study starts with the vigorous literature survey to identify the research gap. After finding the research gap, the first step is to finalize the objectives and methodology. After that, materials for conducting the experimental program is collected. Several trial mixes of lightweight concrete using OPS and POC together have been made. A thorough investigation has been conducted to find the engineering properties of OPS and POC concrete. These engineering properties include the workability, density, compressive strength, splitting tensile strength, flexural strength, and modulus of elasticity. Afterward, 3 meter long rectangular beams have been cast to examine the flexural behavior under two-point static loading. From the experiment, ultimate load carrying capacity has been measured from the Instron Machine, maximum deflection by the Linear Variable Displacement Transducer (LVDT), crack width by the Dino-lite microscope and the strain of beam surfaces by the strain gauge and demec points. These results have been used to analyze the flexural behavior of reinforced PSCC beam comprising failure mode, load- deflection behavior, moment capacity, ductility

characteristic, cracking pattern and steel-concrete strain. The overall research program is summarized in Figure 3.1.
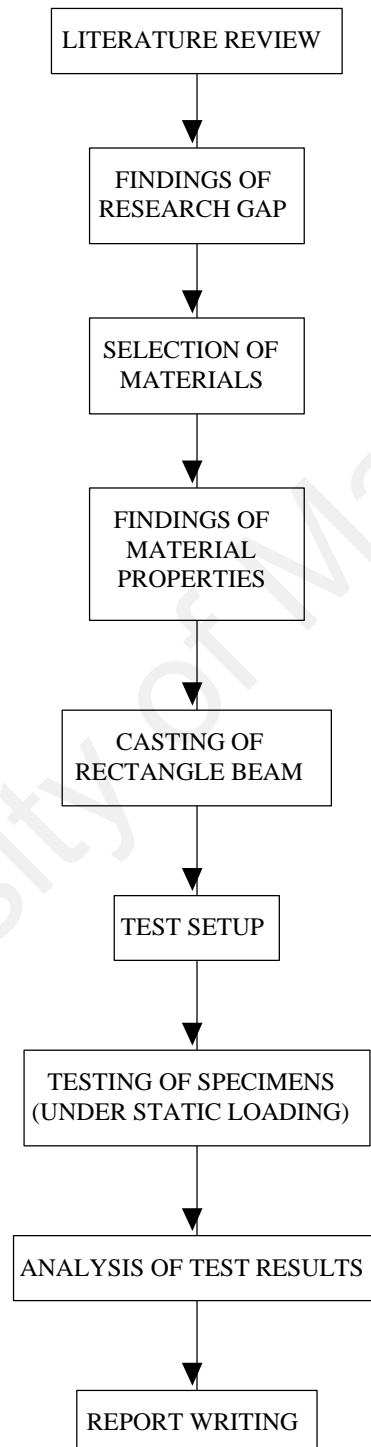
Figure 3.1: Overall research program

3.3 Materials

The engineering properties of newly proposed PSCC and the flexural behavior of reinforced PSCC beam were investigated in this research. To carry out the study of compressive strength and ductility of PSCC, combination of OPS and POC as a coarse aggregate is considered in the concrete mixes. In the subsequent sections, the descriptions of the materials are provided.

3.3.1 Cement

In this study, ordinary Portland cement with a specific gravity of 3.14 g/cm^3 and fineness of 3510 cm^2/g was used as the binder material in the concrete. This cement was collected from the Malaysian market. The compressive strengths of the cement were 34.2 and 45.9 MPa, at 7 and 28 days; respectively.

3.3.2 Fine aggregate

Local mining sand with specific gravity, fineness modulus, water absorption and maximum grain size of 2.68, 2.65, 1.17% and 4.75 mm; respectively, was selected as fine aggregate in the concrete mix.

3.3.3 Coarse aggregates

Two types of coarse aggregates were used in the concrete mix for this study, which was collected from the local palm oil factory in Malaysia as waste materials. Figure 3.2 shows the selected coarse aggregates for producing lightweight concrete. The OPS aggregate is shown in Figure 3.2 (a). OPS aggregate from crushing the larger original OPS aggregate is an appropriate method to enhance the compressive strength of lightweight OPS concrete. After collecting the OPS from the local palm oil industry, it was washed and crushed using a stone-crushing machine in the laboratory. The

flakiness of OPS decreases significantly upon crushing, which improves the performance of the coarse aggregate and yields higher compressive strength. Subsequently, crushed OPS aggregate was sieved using a 5 mm sieve to remove the aggregate less than 5 mm in size. Accordingly, the size of OPS aggregate used was 5 mm and larger. Table 3.1 shows the mechanical properties of crushed OPS.

Figure 3.2: Coarse aggregate (a) OPS aggregate (b) POC aggregate

Another type of coarse aggregate, POC aggregate is presented in Figure 3.2 (b). This POC was also collected from the local palm oil industry in Malaysia. In a similar fashion to OPS, the clinker was crushed and sieved using a 5 mm sieve. As the larger size aggregate has a greater value under the abrasion test, POC retained on the 5 mm sieve was considered to be coarse aggregate. The mechanical properties of POC are also given in Table 3.1.

Table 3.1: Physical and mechanical properties of crushed OPS and POC aggregates

(Mannan and Ganapathy, 2004; Mohammed et al., 2014)

Physical and mechanical properties	OPS	POC
Aggregate size (mm)	5-12.5	5-12.5
Specific gravity (saturated surface dry)	1.17	1.82
Water absorption for 24 h (%)	23.3	4.35
Aggregate abrasion value, Los Angeles (%)	4.8	27.09
Bulk density (compacted) kg/m3	590	781.08
Fineness modulus (F.M)	6.24	6.75
Flakiness index (%)	65.17	-
Elongation index (%)	12.36	-
Aggregate impact value (%)	7.86	25.36

3.3.4 Superplasticizer (SP)

A modified polycarboxylate based water reducer was used as superplasticizer (SP). Sika Viscocrete 2199, which was collected from Sika Kimia Sdn Bhd, Malaysia, was employed as the chloride free SP, in accordance with EN 934-2, and mixed in the concrete at 2.0% of cement weight to facilitate the workability. Figure 3.3 displays the SP used in the test program.

Figure 3.3: Superplasticizer (Sika Viscocrete 2199)

3.3.5 Water

Water is the essential constituent material of concrete for the hydration of cementitious materials and to provide the workability at the time of mixing and placing. Potable water collected from the laboratory water supply system was used for all the mixes, as well as for the purpose of curing. It was visually checked for any dirt and other objectionable elements that may cause color or harm cement hydration. The curing water was changed every month to avoid excessive dirt.

3.3.6 Steel

Deformed steel bars, 12 mm in diameter, were used for internal longitudinal reinforcement in the beams. The deformed bars were tested for tensile strength in the laboratory to confirm the mechanical properties supplied by the manufacturer. The yield stress and modulus of elasticity were found to be 466 MPa and 200 GPa; respectively. As shear reinforcement, 6 mm steel bars with a yield stress of 380 MPa and modulus of elasticity of 200 GPa were used.

3.4 Preparation of concrete sample

For preparing of the concrete sample, at first, several trial mix was performed to finalize the mixing proportion of the desired strength. After that, final mixing was performed to prepare the concrete sample.

3.4.1 Mix proportion

By and large, the LWAC mix design is determined by trial mixes (Shetty, 2005). Most of the previous studies have used 480 to 550 kg/m^3 cement with water cement ratio of 0.3 to 0.4 to get the concrete of compressive strength 30 to 44 MPa (ACI Committee 211.2, 1998; Jang et al., 2015). In this study, 450 kg/m^3 cement content with water

cement ratio of 0.35 is selected for the trial mix. Therefore, this study designs the trial mixes with the optimum cement content for high strength lightweight concrete (LWC) unlike some previous studies (ACI Committee 211.2, 1998). A total of seven trial mixes has been accomplished in the laboratory to obtain grade 45 concrete with a high workability. To achieve workability, SP is added to all the mix. Sieved local mining sand fills the place of fine aggregate.

Moreover, in the mixture, OPS and POC have been used as coarse aggregate in different proportion in the first five trial mixes. In the mix P70, OPS to POC proportion in coarse aggregate was 70% to 30% by volume. This proportion is gradually varied in the successive mixtures as 60% to 40%, 50% to 50%, 40% to 60% and 30% to 70% referred as P60, P50, P40 and P30; respectively. P100 and C100 were incorporated with only OPS and POC respectively. As the OPS aggregate has the lower value of specific gravity, it requires less weight to cover the same volume of concrete. Therefore, P100 mix has the $354kg/m^3$ of OPS aggregate. The specifications of the concrete mixes with the proportions of ingredients are shown in Table 3.2.

Table 3.2: Concrete mix proportions in kg/m^3

Mix ID	Cement	Water	W/C ratio	SP	Sand	OPS	POC
P70	450	158	0.35	2%	1013	248 (70%)	141 (30%)
P60	450	158	0.35	2%	1025	212 (60%)	187 (40%)
P50	450	158	0.35	2%	1158	148 (50%)	195 (50%)
P40	450	158	0.35	2%	1048	142 (40%)	281 (60%)
P30	450	158	0.35	2%	1060	106 (30%)	328 (70%)
P100	450	158	0.35	1%	978	354 (100%)	0
C100	450	158	0.35	2%	1095	0	469 (100%)

3.4.2 Batching procedure

The amount of the constituent materials needed for a batch of concrete were estimated based on the mix proportions. The aggregates, cement, sand, coarse aggregate, water

and SP were taken on the weight basis. To compensate the loss of concrete during mixing and testing, the batch quantity of the fresh concrete was taken 10% more than the required.

3.4.3   Mixing method

A revolving cone type concrete mixture (Figure 3.4) of 100 liters capacity was used in this study to mix the materials. For the preparation of fresh concretes cement, sand, OPS and POC were first loaded into the mixer and blended into a pan mixer for 5 minutes. Then the mixer was stopped. Subsequently, the mixture of SP and about 80% of the water were added into the pan mixture. After 5 minutes of mixing, the remaining 20% of the water was added to the pan mixture, and the mixing continued for another 10 minutes.

Figure 3.4: Concrete mixture machine

3.4.4 Preparation of hardened concrete sample

Immediately after completing the mixing, 100W×100H×100L mm cube, Φ100×200H mm cylinder, 100W×100H×500L mm prism and Φ150×300H mm cylinder specimens were cast in steel moulds. Specimens are compacted using the vibration table. The casting of all the specimens follows BS 1881 (BS, 1997). The specimens have been demoulded after 24 hours and are cured in water at 28 ± 2°C until test days. The 100W×100H×100L mm cube specimens were used to determine the compressive strength. The Φ100×200H mm cylinder specimens were prepared to determine the splitting tensile strength. The 100W×100H×500L mm prism specimens were considered to measure the flexural strength. The modulus of elasticity has been obtained from Φ150×300H mm cylinder specimens. Figure 3.5 Shows the steel molds which were used to cast the concrete sample.

Figure 3.5: Steel moulds

3.5   Testing of hardened concrete

The hardened concrete was tested for the compressive strength, splitting tensile strength, flexural strength, modulus of elasticity and stress-strain behavior, which are discussed in subsequent sections.

3.5.1   Compressive strength test

The compressive strength test was determined according to BS 1881: Part 116 (BS, 1997) using triplicate 100×100×100mm cube specimens. The specimens were tested at the ages of 1, 3, 7 and 28 days. An ELE (Engineering Laboratory Equipment) testing machine with load capacity 2000 kN was used in the compression test and the loading rate was 2.4 kN/s. The maximum crushing load of the specimen was obtained from the compression machine. An operational stage of the compressive strength is shown in Figure 3.6.
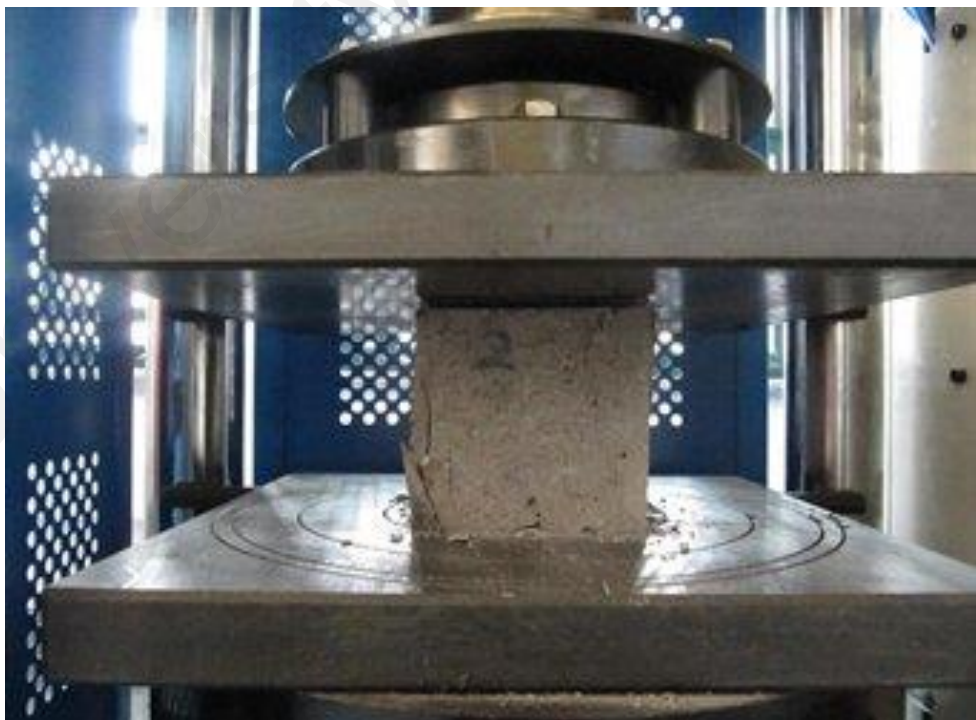
Figure 3.6: Compressive strength test

Analytically, the compressive strength f_c (MPa or N/mm²) was calculated by dividing the crushing load by the contact surface area of the test specimen, as shown in Equation 3.1.

$$f_c = \frac{F_c}{A_c} \qquad\qquad 3.1$$

where,

F_c = Crushing load (N)

A_c = Contact area of specimen (mm²)

3.5.2 Splitting tensile strength test

The splitting tensile strength test was carried out according to BS 1881: Part 116 (BS, 1997) using triplicate Φ100×200H mm cylinder specimens. The values were taken at the ages of 3, 7 and 28 days. In this test, the specimen was positioned on the centering jig with packing strip placed along the top and bottom diametrical faces. The load was applied and increased continuously at a rate of 1.767 kN/s until failure. An operational stage of the splitting tensile strength is shown in Figure 3.7.

The splitting tensile strength f_t (MPa or N/mm²) was calculated using the Equation 3.2.

$$f_t = \frac{2Fm}{\pi \times L \times d} \qquad\qquad 3.2$$

where,

F_m = Maximum load (N)

L = Length of specimen (mm)

D = Diameter of specimen (mm)

Figure 3.7: Splitting tensile strength test

3.5.3 Flexural strength test

The flexural strength test followed BS 1881: Part 116 (BS, 1997) using $100W \times 100H \times 500L$ mm prism specimens. The testing ages were 3, 7 and 28 days. The flexural strength was determined by applying a constant moment at the central zone of the specimen using a two-point loading using EL 33-6090 flexural testing machine manufactured by ELE Ltd. The load was applied steadily and continuously at the rate of 0.067 kN/s until failure. An operational stage of the flexural strength is shown in Figure 3.8.

The flexural strength, also known as modulus of rupture, f_r (MPa or N/mm^2) was calculated using the Equation 3.3.

$$f_r = \frac{F_b \times L}{b \times d^2}$$
3.3

where,

F_b = Breaking load (N)

L = Distance between the support roller (mm)

b = Width of the cross section (mm)

d = Depth of the cross section (mm)

Figure 3.8: Flexural strength test

3.5.4 Static modulus of elasticity test

The static modulus of elasticity test was conducted at the ages of 28 days according to BS 1881: Part 116 (BS, 1997). Triplicate cylinder specimens (Φ150$\times$300H mm) were used at testing age. The test specimen was placed centrally in ELE compression testing machine with the strain measuring apparatus attached axially. The specimens were loaded at least twice. The load was applied continuously without any shock. The initial load corresponding to the longitudinal strain of 50 millionths was observed. The stress was steadily increased at a constant rate of 0.6 N/mm^2.s^{-1} until an upper loading stress equaled to 40% of the cylinder compressive strength was reached, and the strain gauge

reading was taken. An operational stage of the static modulus of elasticity is shown in Figure 3.9.

The static modulus of elasticity, E_s (MPa or N/mm^2) was calculated using the Equation 3.4.

$$E_s = (S_2 - S_1) (\varepsilon_2 - 0.000000344) \qquad 3.4$$

where,

E_s = Static modulus of elasticity, GPa

S_1 = Stress corresponding to a longitudinal strain of 50 millionths, MPa

S_2 = Stress corresponding to a 40% ultimate load, MPa

ε_2 = Longitudinal strain produced by stress

Figure 3.9: Static modulus of elasticity test

3.6 Experimental program for flexural behavior of PSCC beam

3.6.1 Beam reinforcement fabrication

In this study, eight PSCC rectangular beam specimens were fabricated and tested. All the specimens were designed as under reinforcement according to EC2 (2004). The specimens were singly reinforced with three varying reinforcement ratio (ρ). Each reinforcement ratio has two numbers of beam samples. All specimens have the rectangle geometry with a cross-sectional area of 150 mm $\times$ 250 mm and the length of the specimens was 3300 mm. Beam size and length were chosen to conduct typical flexural failure. Therefore, effective span and shear span were selected as 3000 mm and 1150 mm, respectively. The concrete clear cover for all the beams was kept constant at 30 mm. The internal tension and hanger reinforcement of all beams were bent ninety degrees at both ends to fulfill the anchorage criteria. Two 10 mm diameter deformed hanger bars at the compression zone were used up to shear span zone. 8 mm diameter plain steel bar was used as shear reinforcement and distributed only in the shear span to ensure the flexure failure of PSCC beams. Dimensions and reinforcement details of specimens are shown in Table 3.3 and Figure 3.10.

Table 3.3: Reinforced PSCC beam details

Beam ID	Beam Size b $\times$ d (mm)	Tensile steel bar size	Tensile steel area (mm^2)	$\rho = 100\ A_s/bd$ (%)
1B	150 x 250	2-Φ10mm	158	0.50
2B	150 x 250	2-Φ12mm	226	0.72
3B	150 x 250	2-Φ12mm	226	0.72
4B	150 x 250	3-Φ12mm	339	1.09
5B	150 x 250	3-Φ12mm	339	1.09
6B	150 x 250	2-Φ16mm	402	1.30
7B	150 x 250	2-Φ16mm	402	1.30
8B	150 x 250	2-Φ12mm+2-16mm	628	2.11
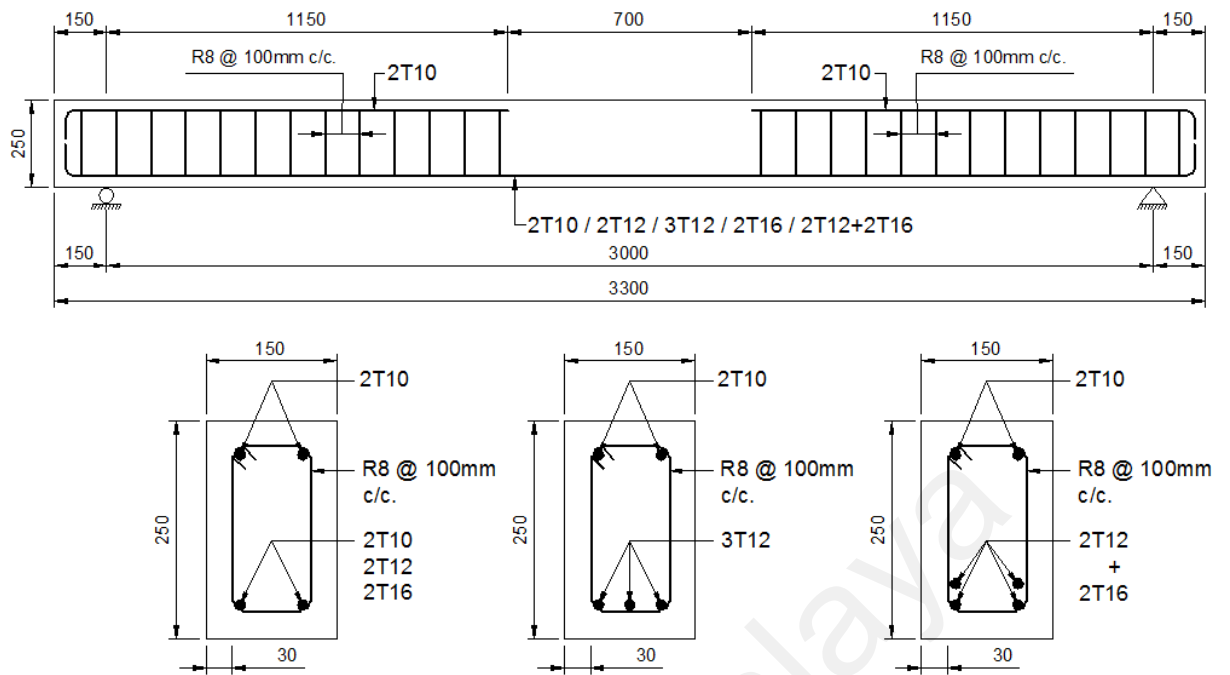
Figure 3.10: Reinforced PSCC beam details

3.6.2 Formwork

Fresh concrete, being plastic requires some kind of formwork to mould it to the required shape and also to hold it till it sets. The formwork has, therefore, got to be suitably designed. In this study, the formwork used for casting of all the specimen consists of mould prepared with two channel sections bolted steel plate with both ends closed by plywood. The formwork was thoroughly cleaned and all the corners and junctions were properly sealed by silicon sealer to avoid leakage of concrete through small openings. After that, shuttering oil was applied to the inner face of the formwork. Finally, the reinforcement cage was placed in position inside the formwork carefully keeping in view a clear cover of 30 mm the top, bottom and both sides.

3.6.3 Mixing of concrete

The hardened concrete properties of seven mixtures are presented in Table 3.2. From this tabular sketch, it is being observed that P50 exhibit the maximum compressive strength (46 MPa) and other mechanical properties are better among the mixes. Hence, P50 was selected for the beam casting. Same batching and mixing method used in the investigation of materials properties was followed to investigate the flexural behavior of reinforced PSCC beams.

3.6.4 Concrete compaction

All specimens were compacted by using a vibrating needle (Concrete vibrator: Robin EY20-3C). Figure 3.11 shows the vibrating needle used in compacting concrete. Sufficient care was taken to avoid any displacement of the reinforcement inside the formwork. Finally, the surface of the concrete was leveled and smoothened by a metal trowel.

Figure 3.11: Vibrating needle

3.6.5 Curing of beam

The concrete is cured to prevent the loss of water which is essential for the process of hydration as well as for hardening. Moreover, curing prevents the exposure of concrete to the hot atmosphere which may lead to quick drying out of moisture in the concrete and thereby it subjects shrinkage crack in the immature concrete. Curing was done by spraying water on the foam sheet over the beam surface. The curing was started as soon as the concrete is sufficiently hard and it continued till 28 days. After 28 days, beams were stored for the flexural testing.

3.7 Instrumentation

3.7.1 Strain gauge

During the fabrication of steel cage, two TML strain gauges (model: FLA- 10-11) were fixed with both reinforcements for measuring tensile strain. To facilitate strain gauges, a small part of tensile reinforcement at mid-span of beams were grounded to smooth, strain gauge was attached to the tensile steel with adhesive and there were provided a protective layer using silicone gel to avoid any accidental damage during concreting. Figure 3.12 and Figure 3.13 show the steps of attaching strain gauge to the steel reinforcement.

Figure 3.12: Surface preparation of steel bars to place strain gauges

Before testing, the beam was whitewashed, and the location of neutral axis and center lines were marked. The compressive strains of concrete were also measured through strain gauges (model: FLA- 30-11). These strain gauges were attached to the top surface of the concrete beam as well. The surface was smoothed and an adhesive layer applied to attach the strain gauge.

Figure 3.13: Strain gauges covered with silicone gel

3.7.2   Support condition and instron universal machine

The PSCC beams were simply supported and tested under two-point loading as shown in the Figure 3.18. An instron universal testing machine of the capacity of 500 kN with built-in load cell was used in the testing. It has both manual and automatic controls and the options of load or position controls could be used in testing of the beam. The load from the actuator was transferred to the beam using a steel spreader beam. All the beams were loaded under same loading criteria that loads were kept at 700 mm apart on a span of 3000 mm.

3.7.3 Vertical linear variable differential transducer and data logger

The deflection of the specimens was measured at mid-span of the beam specimen by using an LVDT. All the data from the load cell, LVDT and strain gauge were recorded by a data logger at every 10-second intervals. Figure 3.14 shows the data logger used in the experiment to record the data.

Figure 3.14: Data logger TDS-530

3.7.4 Dino-lite digital microscope

The crack widths at the level of tensile reinforcement of the selected beam specimens were measured using a hand-held microscope (dino-lite digital microscope) with a sensitivity of 0.02 mm. Figure 3.15 shows the dino-lite digital microscope for crack width measurement.

Figure 3.15: Dino-lite digital microscope for crack width measurement

3.7.5 Demec Points

Demec points were installed on the side surfaces of each concrete beam to measure strain and to determine the position of the neutral axis of the beam sections. The distance between two horizontally placed Demec points was 200 mm. The concrete surface where each Demec point was to be installed was ground to ensure proper bonding. The surface was then cleaned with acetone to remove dust. After preparing the concrete surface, the Demec points were installed using an adhesive as shown in Figure 3.16 and allowed to set for at least 24 hours.

Figure 3.16: Demec points on a concrete beam

3.7.6 Digital Extensometer

The bending deformation of each beam under loading was measured from its Demec points using a digital extensometer (Figure 3.17). This was used to estimate the strain profile of each beam and to determine the position of the neutral axis. The attachment of Demec points on the side surface of beam specimens is described in the previous section.

Figure 3.17: Digital extensometer

3.8 Testing method

Before testing, the beam was checked dimensionally, and all the necessary information were recorded carefully. After setting the required instruments such as strain gauge, LVDTs, Data logger, etc., the beams were preloaded with an approximate minimal force of 0.5 kN to allow initiation of the LVDT and strain gauges. Then, the tests were conducted using two types of control. Initially, load control option was used until the yield capacity of the specimens and, then, displacement control option was used until failure of the specimens. The rate of the actuator was set as 2 kN/min during load

control and 2 mm/min during displacement control. All the reading were recorded using data logger at 10-second intervals. In addition, the strain distribution on the vertical face of the beams in the flexural zone was determined using demec points. Demec reading was taken at every 5 kN interval during load control option using a de-mountable digital extensometer with a sensitivity of 0.001 mm. The first crack load was noted at the immediate formation of the first crack and all the cracks were marked as and when they propagated in the beam. Figure 3.18 shows the experimental arrangement for the Beam specimens
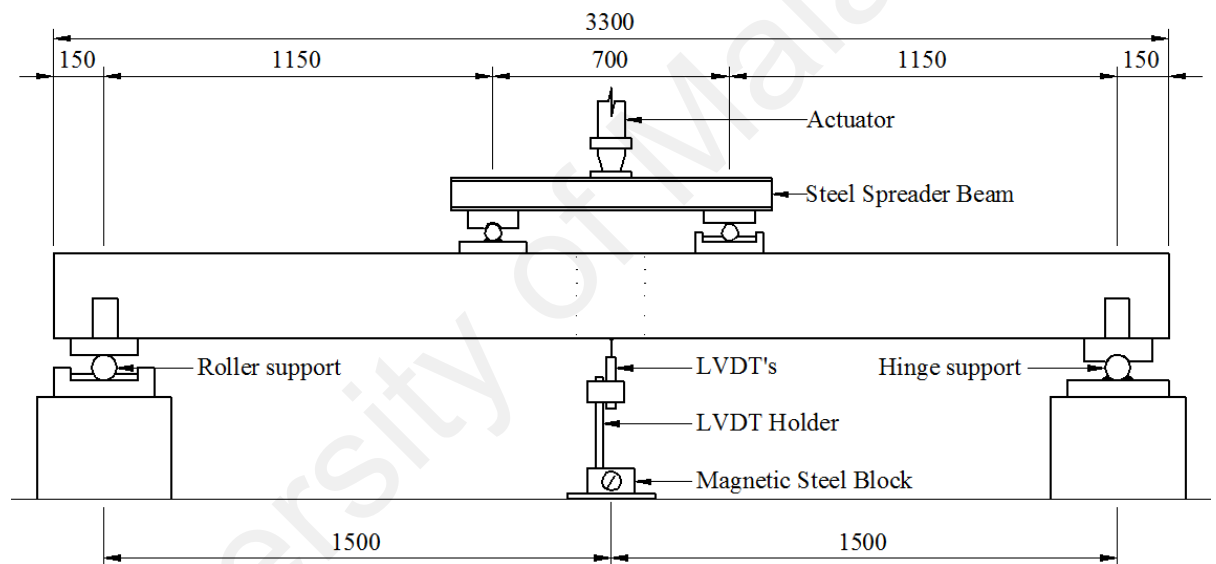
Note: All dimensions are in mm

Figure 3.18: Experimental arrangement for the Beam specimen

CHAPTER 4: RESULTS AND DISCUSSIONS

4.1 Introduction

This chapter presents the results and critical discussions of this study. Experimental results of fresh and hardened properties of PSCC have been discussed here. The effects of the combination of OPS and POC content as a coarse aggregate on the PSCC is also highlighted. The deflections, the failure mechanisms, and the ultimate failure loads of all the PSCC beam specimens are also reported and discussed with critical evaluation.

4.2 Engineering properties of PSCC

The engineering properties of PSCC concrete are investigated initially. OPS and POC mixture as a coarse aggregate has been considered in the concrete mixes to find the engineering properties. In this succeeding sections, the description of the material properties is given elaborately.

4.2.1 Workability

The results for the workability of PSCC are presented in Figure 4.1. Mehta and Monteiro (2006) suggested that for structural lightweight concrete, slump value of 50 to 75 mm may be sufficient to obtain workability that is similar to a 100 to 125 mm slump for normal weight concrete. All the trial mixes show acceptable workability. As the water-cement ratio and the usage of SP were kept constant, slump values for all the mixes are in the same range. The slump value of all mixes ranged from 50 mm to 70 mm. This range is very acceptable in the lab condition. Nevertheless, the compaction of all mixes under vibration was satisfactory. All the coarse aggregate were taken as saturated surface dry condition (SSD). Therefore, in measuring the slump value, no influences of coarse aggregate has been observed. In this experimental program, mixes

having slump value within the acceptable limits indicate the acceptable performance of the PSCC in a real application.
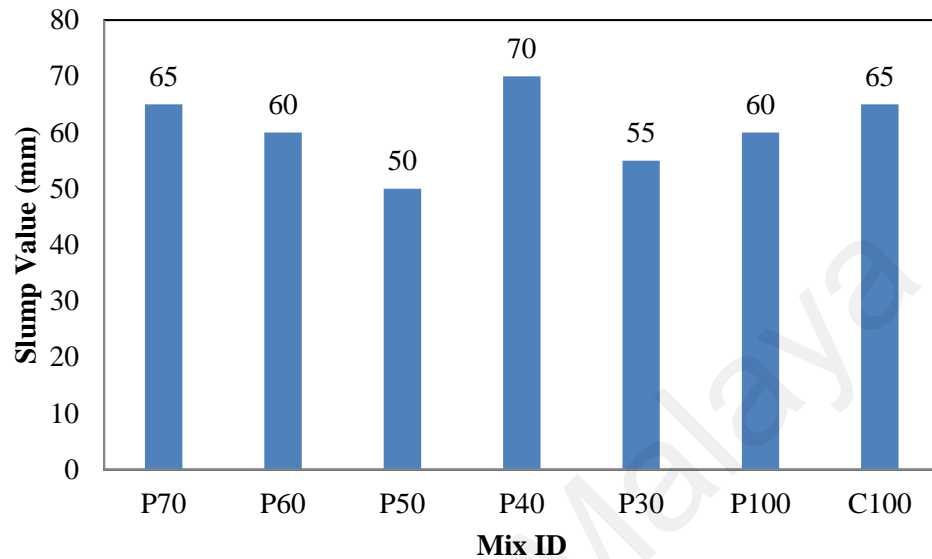
Figure 4.1: Slump values for different mixes.

4.2.2 Density

Structural lightweight concrete has the oven dry density less than 2000 kg/m^3 (Newman and Choo, 2003). From Table 4.1, it can be seen that densities of all mixes are within the range of structural LWC. The 28- day air dry density and oven dry density of PSCC are in the range from 2060 to 2160 kg/m^3 and 1888 to 1991 kg/m^3, respectively. Assuming the density of normal weight concrete (NWC) is 2400 kg/m^3, the 28-day air dry density and oven dry density of PSCC are 10% to 14% and 16% to 19% less than the ordinary concrete respectively. From the Table 4.1, it also can be seen that with the increase of POC content in the concrete, density of concrete increases as the POC aggregate has higher value of specific gravity than OPS aggregate.

Table 4.1: Densities at different condition

Mix ID	Density (kg/m³)	
	Air-dry density	Oven-dry density
P70	2083	1951
P60	2115	1991
P50	2145	1960
P40	2130	1970
P30	2140	1980
P100	2060	1888
C100	2160	1990

4.2.3   Compressive strength

Table 4.2 shows the 28-days compressive strength development for all the mixes. The test result shows that with the increase of the percentage of OPS in the combination of coarse aggregate, the 28-days compressive strength decreases. P50 shows maximum value for the 28-day compressive strength of 46.47 MPa and it is 30% higher than that of P100. P70 exhibits the lowest value for the 28-day compressive strength. From the tabulated data, it can be found that 100% replacement of OPS with POC aggregate increases the compressive strength about 15% whereas half of the OPS replacement caused 30% increase in compressive strength. In P70, OPS content goes up to 70%, resulting 18% drop in the compressive strength compared to that of P50. This weakening can be attributed to the round and plain surface texture of OPS which imparts poor bondage to concrete if present excessively. POC aggregate, on the other hand, is rough and porous, induces strong bonding with cementing paste. Concrete containing 100% of OPS (P100) poses the lowest compressive strength. On the other hand, concrete containing 100% of POC (C100) shows the compressive strength of 41 MPa.

In this study, PSCC was prepared using a mixture of crushed OPS and POC as coarse aggregate in different mix proportions. Therefore, their correlation between the initial

age (1-day, 3-day, and 7-day) compressive strength and 28-day compressive strength are shown in Figure 4.2. Usually, the linear correlation gives high values of R^2 between the initial and 28-day compressive strength. Lo et al. (2004b) reported values of R^2 between 82 to 90% for the correlation between 28-day compressive strength and the 7-day compressive strength for LWAC using expanded clay which is similar to this study (R^2 = 85 to 95%). The equations show the relationship between 1-day against 28-day, 3-day against 28-day and 7-day against 28 day compressive strengths:

$$(f'_{c28}) = 0.7847f'_{c1} + 18.907 \tag{4.1}$$

$$(f'_{c28}) = 0.7161f'_{c3} + 15.727 \tag{4.2}$$

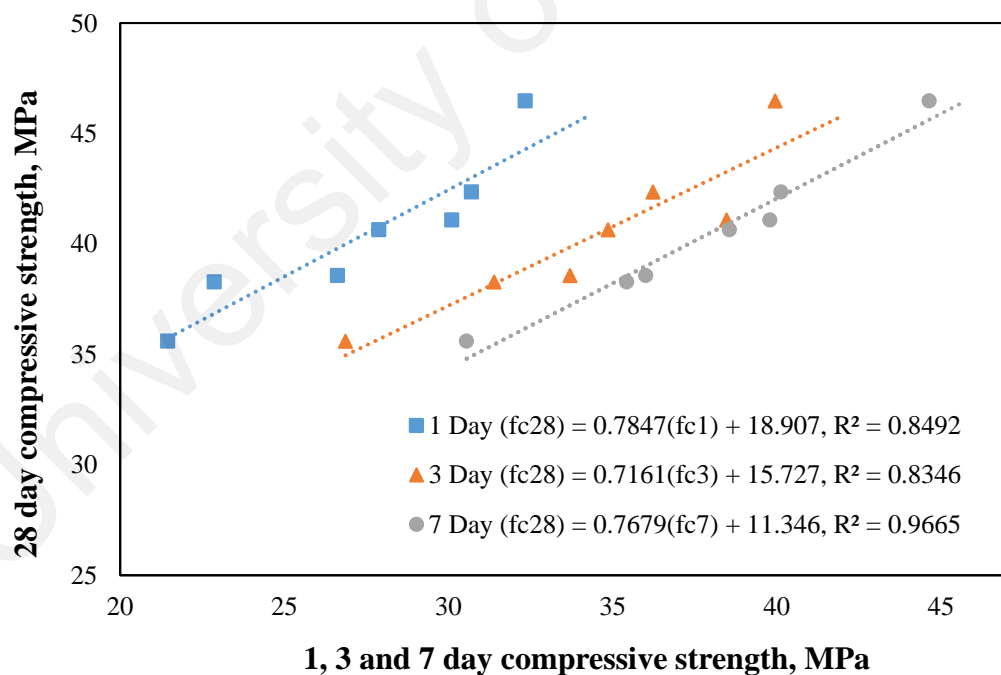$$(f'_{c28}) = 0.7679f'_{c7} + 11.346 \tag{4.3}$$

Figure 4.2: Relationship of early age (1-day, 3-day and 7-day) compressive strength with 28-day compressive strength.

It is a great merit of the POC aggregate that it has a rough surface which helps to create stronger bonding with cement paste. The crushing of aggregate in compressive test indicates good bonding between mortar and aggregates. On the other hand, POC aggregate is porous in nature. For this reason, some cementing material enters into these pores and left over mortar may not be sufficient to cover the total surface area of coarse aggregate. Eventually, it decreases overall bonding strength (Ahmmad et al., 2014). However, an optimum mix is expected which ensures better bonding and 28-days compressive strength. P50 may refer to the optimum mix ratio in this study.

Table 4.2: Compressive Strength of OPS and POC concrete

Mix ID	Compressive Strength (MPa)			
	1 day	3 day	7 day	28 day
P70	22.87	31.39	35.43	38.28
P60	26.62	33.70	36.01	38.57
P50	32.34	39.95	44.64	46.47
P40	30.70	36.23	40.13	42.35
P30	27.88	34.86	38.56	40.64
P100	21.45	26.86	30.55	35.60
C100	30.10	38.47	39.79	41.08

4.2.4 Splitting tensile strength and flexural strength

The measured splitting tensile and flexural strengths for all the mixes are illustrated in Table 4.3. From the tabular sketch, it is seen that the minimum 28-days splitting tensile strength is 2.8 which fulfills the minimum requirement (2.0 MPa) for lightweight concrete (Kockal and Ozturan, 2011). P50 has the highest value of splitting tensile (3.67 MPa) and flexural strength (6.0 MPa) over the control mixes P100 and C100. On the other hand, minimum 28-days flexural strength is found as 3.93 MPa. About 80 to 90% of both the splitting tensile and flexural strength have been developed in first 7-

days. Therefore, splitting tensile and flexural strength of structural member made from these lightweight aggregate concretes can be exploited at an early age (7-days). It can be comprehended that different equations are required for lightweight concrete made from the different aggregate. Figure 4.3 shows the relationship between the compressive strength (f_c) and the splitting tensile (f_t) and flexural strengths (f_r) of PSCC. From the Figure 4.3, equations have been suggested to predict splitting tensile and flexural strengths. Equation 4.4 and 4.5 represents the splitting tensile strength and the flexural strengths, respectively.

$$f_t = f_c^{1.0126} \tag{4.4}$$

$$f_r = f_c^{2.2401} \tag{4.5}$$

Table 4.3: Flexural and splitting tensile Strength of OPS and POC concrete

Mix ID	Splitting tensile Strength (MPa)			Flexural Strength (MPa)		
	3 day	7 day	28 day	3 day	7 day	28 day
P70	2.41	2.76	2.90	3.71	3.75	3.93
P60	2.36	2.75	3.02	3.98	3.85	4.33
P50	3.38	3.53	3.67	5.18	5.83	6.00
P40	2.86	3.14	3.37	4.77	5.21	5.47
P30	2.32	2.52	3.11	4.04	4.15	4.27
P100	2.50	2.76	2.86	2.93	3.03	3.34
C100	2.79	3.00	3.25	4.00	4.44	4.69

From Table 4.3, the influence of a combination of OPS and POC coarse aggregates in the PSCC can be observed. It is perceived that, with the increased percentage of OPS aggregate, splitting tensile and flexural strength is decreased. When the POC content is gradually increased the splitting tensile and flexural strength also increased. After the ratio, 50% of OPS and 50% of POC aggregate mix (P50), both the splitting tensile and flexural strength tend to drop. Because the round surface of OPS aggregates poses the weaker bond in concrete and the POC aggregate is porous in nature which allows some

cementing material entering to the pores. Eventually, it decreases overall bonding strength as supported in the study of (Ahmmad et al., 2014). Therefore, P50 may be the optimum mix which ensures the maximum splitting tensile and flexural strength.
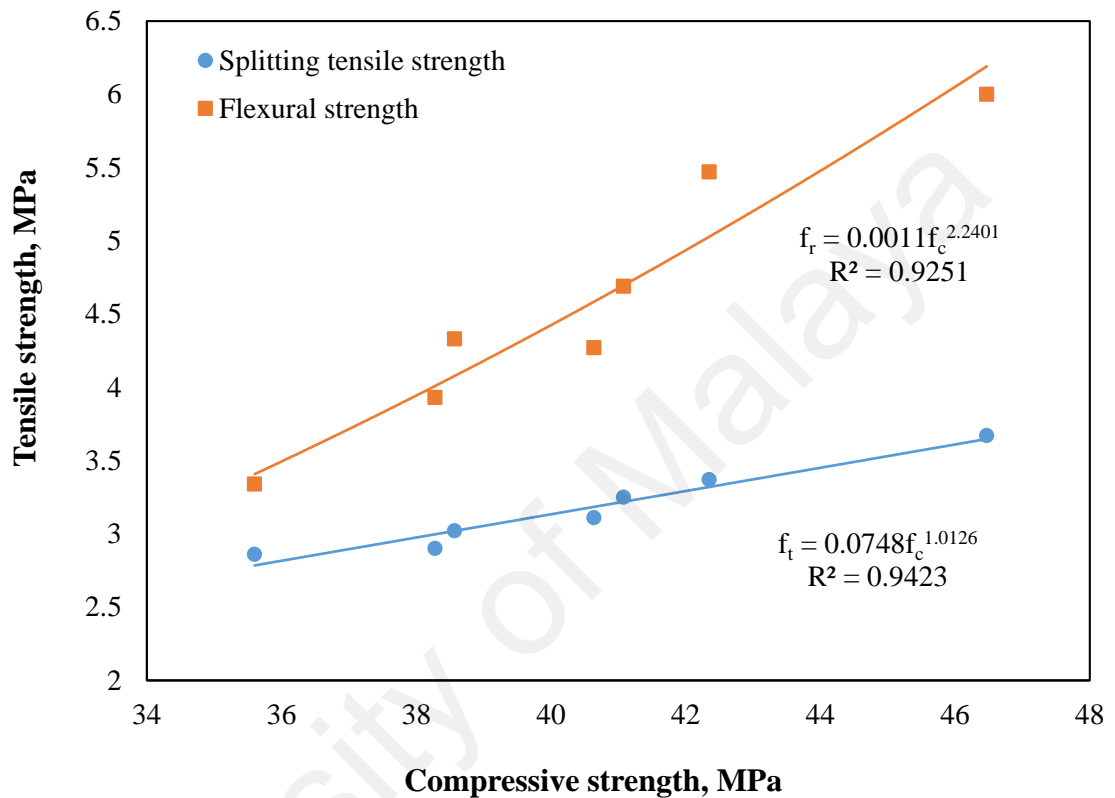
Figure 4.3: Relationship between 28-day compressive and splitting and flexural strength of PSCC

4.2.5   Modulus of elasticity

For calculating the deflection and the stiffness of any structural element, modulus of elasticity (MoE) is one of the most important characteristics. Therefore, it is necessary to find a suitable correlation depending on the compressive strength for predicting the MoE. The elastic modulus of concrete depends on the modulus of elasticity of its components and their proportions (Neville, 1970). With the increase of POC aggregate contents in the LWC mix, the modulus of elasticity increases as shown in Figure 4.4.

This increase results from the high specific gravity of POC content. The mixture P50 gives the maximum value of modulus of elasticity, whereas P40 shows 6% lower value of modulus of elasticity. On the other hand, when the mixes contain POC lower than 50% by volume (P60 and P70), the modulus of elasticity dips down to 20%.

Figure 4.4 shows a relationship between the MoE and the cube compressive strength of PSCC comparing with the equations (Equation 4.6) used previously to predict the MoE of lightweight concrete in CEP/FIP manual (Short and Kinniburgh, 1978). Figure 4.4 also compares empirical equations (Equation 4.7 and 4.8) suggested by previous researchers to predict the MoE for OPS concrete. But none of them are suitable for all type of LWAC (Ahmmad et al., 2014; Alengaram et al., 2011b).

$$E_{s(pre)} = [\omega/2400]^2 \times f_c^{1/3} x9.1 \qquad (4.6)$$

$$E_{s(pre)} = [\omega/2400]^2 \times f_c^{1/3} x5.0 \qquad (4.7)$$

$$E_{s(pre)} = 0.0005 \times f_c^{2.69} \qquad (4.8)$$

where, $E_{s(pre)}$ (GPa) is the predicted elastic modulus, f_c (MPa) is cube compressive strength and ω (kg/m^3) is the air dry density of concrete.

From Figure 4.4, it is observed that CEB/FIP manual highly overestimates the MoE for the PSCC. The equation derived by the Alengaram et al. (2011b) also overestimates the MoE for the PSCC. The Equation derived by the Ahmmad et al. (2014) overestimates to the MoE for the PSCC which contains a high amount of POC content. From the above experimental findings, a simplified equation (Equation 4.9) is proposed to predict the MoE for the PSCC based on the 28-day compressive strength.

$$E_{s(pre)} = 0.0261 \times f_c^{1.6167} \qquad\qquad\qquad\qquad (4.9)$$

where, $E_{s(pre)}$ (GPa) is the predicted elastic modulus and f_c (MPa) is cube compressive strength.
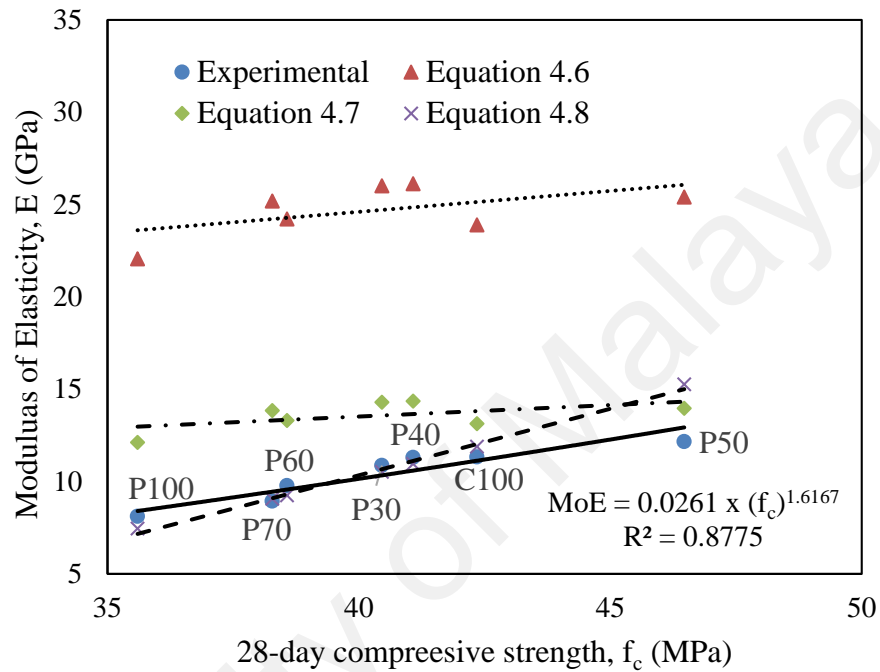
Figure 4.4: Compressive strength vs. Modulus of Elasticity.

4.2.6   Ultrasonic pulse velocity and compressive strength

There is no distinctive correlation with ultrasonic pulse velocity (UPV) and the compressive strength of the concrete (Neville, 2008). The UPV values are greatly influenced by the mixture composition of concrete, water/cement ratio, type and period of curing, and subsequently compressive strength. When the voids are filled with water, the UPV travels faster than when the voids are filled with air, which indicates that the moisture also affects the UPV of the concrete (Neville, 2008). The concrete with UPV values between 3.66 and 4.58 km/s is termed as 'good' (Leslie and Cheesman, 1949). Hence, it is considered that the concrete has no large voids or cracks to reduce the

structural integrity. The UPV values for all the mixes investigated in this research were found higher than 3.66 km/s. The relationship between the compressive strength and UPV of the PSCC has been developed. Figure 4.5 shows a correlation between the 28-day compressive strength and UPV of the PSCC mixes. From the figure, following empirical equation (Equation 4.10) is developed:

$$f_c = 5.0658 \times (UPV)^{1.4502} \tag{4.10}$$
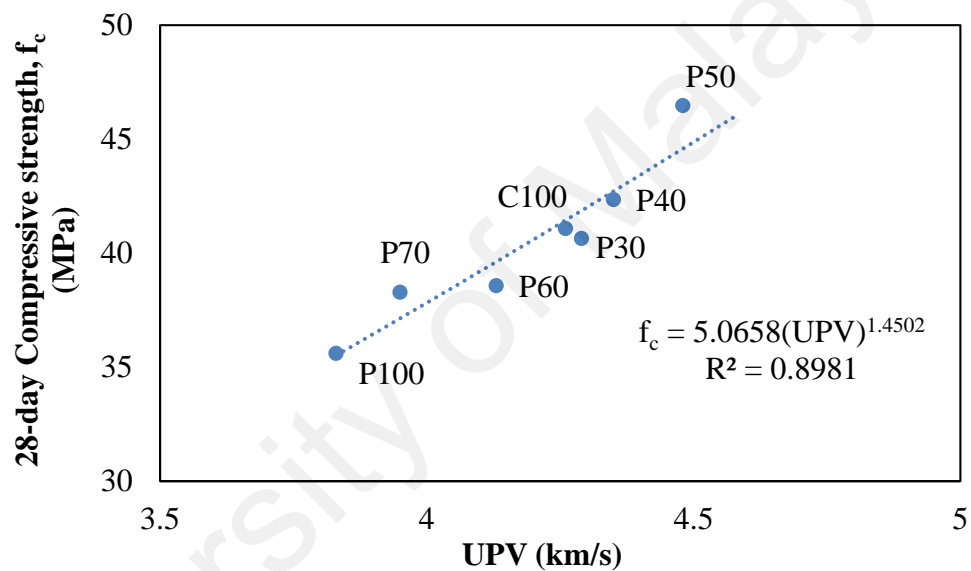
Figure 4.5: 28-day compressive strength vs. UPV of PSCC

4.3 Stress-strain and ductility behavior of PSCC

4.3.1 Stress-strain behavior

Figure 4.6 shows the stress–strain curves of the tested samples containing different percentages of OPS and POC mixture. Both vertical and lateral strains are plotted against the applied compressive load. The vertical displacement is shown in positive X-axis and lateral displacement at negative X-axis in Figure 4.6. The stress–strain curves of PSCC samples softens towards a rounded peak at the post-yield stage. Moreover, there is a very slow dropping tendency after post yield, mainly because the PSCC

concrete has a good interlocking (Ahmmad et al., 2014) and a bilinear ductile (Shafigh et al., 2012) stress–strain behavior. The PSCC concrete specimen can undergo larger deformation before failure, and such a failure is ductile and gives warning of the impending failure similar to steel. For P50 and P40, the strains at maximum stress were measured 0.0028 and 0.0034, respectively and is less than that of for P70 and P60 (0.0035 and 0.0040, respectively), which are near to the recommended range of lightweight concrete element (Turatsinze and Garros, 2008). The recommended range is 0.026–0.003. With the increase of POC aggregates in the concrete, strain at maximum stress exhibits the lower value and vice versa with the increase of OPS aggregates. It is also observed that concrete with POC aggregates shows less ductile behavior with maximum stress value. However, OPS concrete revealed the good ductile behavior with maximum stress value. After combining the OPS and POC coarse aggregates in the concrete, the moderate ductile behavior is found with higher stress value. From the test results, calculated Poisson's ratio of PSCC is 0.21 which is in good agreement with the requirement of concrete.
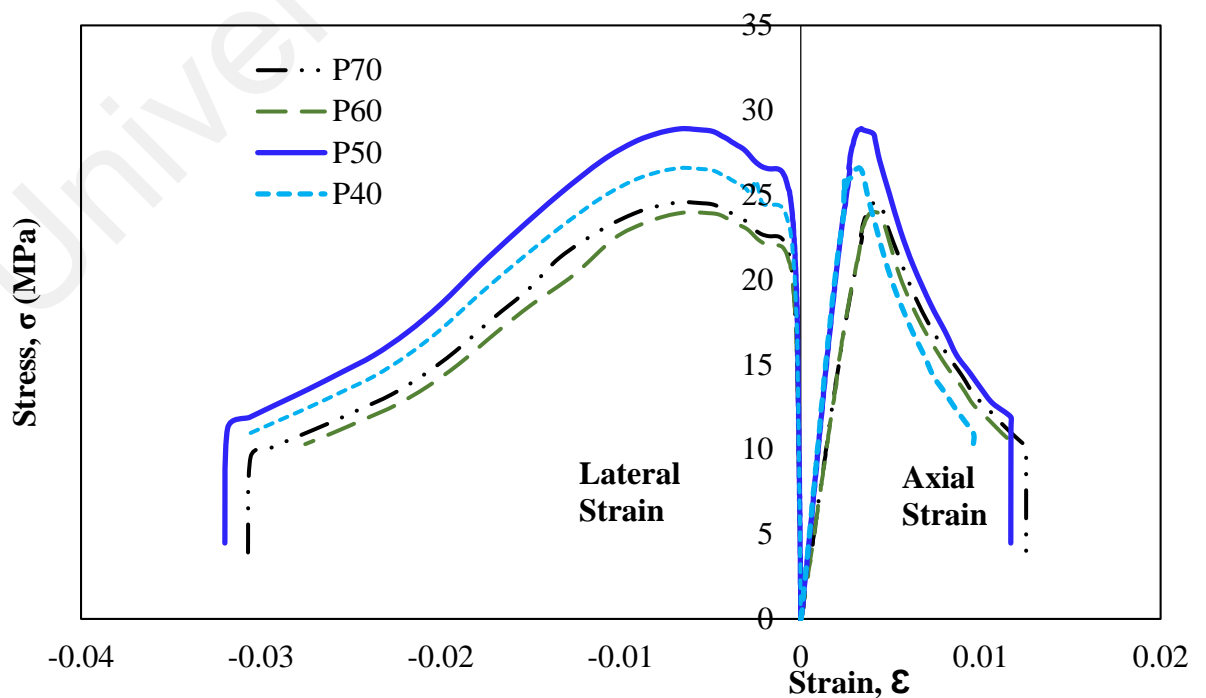
Figure 4.6: Stress-strain curves for vertical and lateral displacement.

4.3.2 Ductility performance

The ductility indices of PSCC obtained from the laboratory results are presented in Table 4.4. The compressive strength, modulus of elasticity and corresponding ductility indices are shown in the table. Also, the concept of ductility indices is defined graphically in Figure 4.7. The ductility of any structural element is usually specified as the capacity of the structural element to undergo load still experiencing extra distortion beyond the maximum load stage (Ahmad et al., 1995). This definition is qualitative and a measure of the displacement ductility of critical compression elements. The ratio of the area under the stress-strain curve up to $5\varepsilon_o$ to the area up to ε_o for displacement is defined as the ductility index (μ), as shown in Figure 4.7.
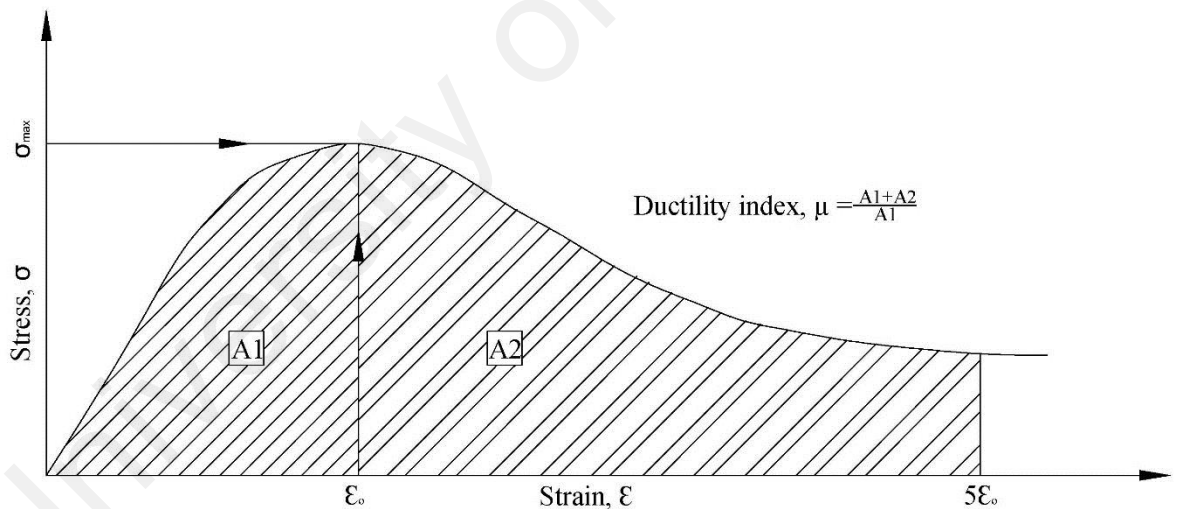
Figure 4.7: Diagram for a description of displacement ductility.

The displacement ductility values stated in this study are the strain ductility of the compression-critical member. Here, ε_o is the strain at peak stress (σ_{max}) for the concrete element. Members with the displacement ductility ratios in the range of 3 to 5 can be taken for structural elements subjected to vast displacements (Ashour, 2000). From the tabular sketch, it is seen that all the mixing fall in the range of requirement for the

structural element. With the increase of OPS content in the concrete mix ductility of concrete increases which supports existing literature (Ahmmad et al., 2014). Therefore, it can be stated that mixing OPS with POC in the concrete produces ductile concrete with higher compressive strength. Among the mixes in this study, P50 shows acceptable ductility with maximum compressive strength.

Table 4.4: Displacement ductility indices of PSCC for different mixture

Mix ID	Compressive strength (MPa)	Elastic modulus (GPa)	Displacement ductility		
			Stress	Strain	μ
P70	38.28	8.93	24.00	0.00408	3.82
P60	38.57	9.77	24.57	0.00422	3.67
P50	46.47	12.16	28.92	0.00338	3.56
P40	42.35	11.33	26.60	0.00324	3.26

4.4 Flexural behavior of reinforced PSCC beam

In this section, the results found from the experimental program of eight PSCC beams cast with the optimum mix of OPS and POC coarse aggregates have been presented with the critical discussion.

4.4.1 Failure mode

Observed failure mode was pure flexural for all beams. Figure 4.9 and Figure 4.9 shows the mode of failure of the tested beam specimens. As all the beams were designed as under-reinforced beams, yielding of tension steel occurred first. Then this was followed by the crushing of concrete at the compression zone. Such behavior was expected for the flexural failure.
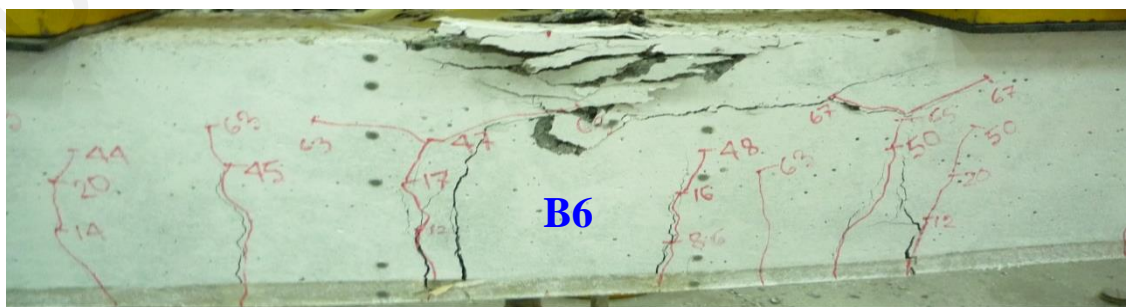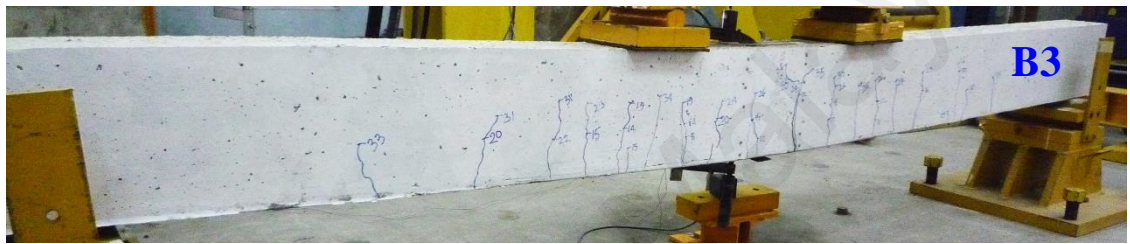
Figure 4.8: Typical flexural failure of the Beam specimen (B1 to B6)
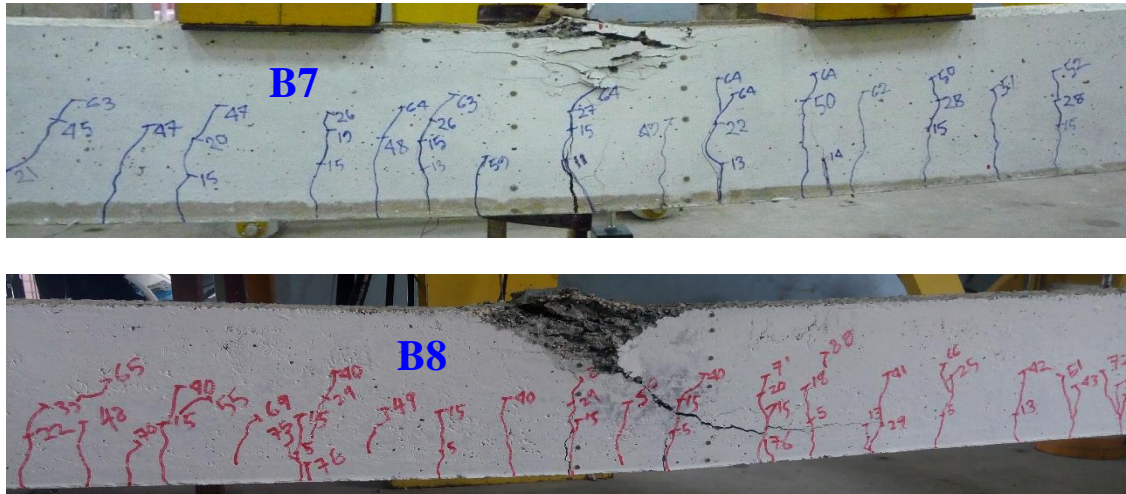
Figure 4.9: Typical flexural failure of the Beam specimen (B7 to B8)

The experimental program also confirmed substantial deflection before the ultimate failure of the beam. To ensure the typical flexural failure, no compression reinforcement was provided in the bending zone, and the stirrup spacing was kept as 100 mm center to center in the shear region only. So failure took place with a flexural crack in the bending zone and the crack was propagated to the neutral axis. After that, all the cracks started to be inclined to the middle of the beam to create the compression zone. Then the gradual crushing of concrete occurred in this zone. The concrete crushing depth was varied from 35 mm to 55 mm. Figure 4.10 also shows the enlarged concrete crushing zone. General observation shows that the performance of reinforced PSCC beams is analogous to that of other LWC prepared from OPS, POC and coconut shell as reported by (Gunasekaran et al., 2013; Mohammed et al., 2014; Teo et al., 2006b).

Figure 4.10: Concrete crushing and Cracks of Beam specimens at constant moment

zone

4.4.2 Load-deflection behavior

Figure 4.11 shows the experimental load-deflection curves at mid-span for the tested eight singly reinforced beams. It is being observed that before the first crack occurred, the slope of the load-deflection curve was steep and linear. After forming the first flexural cracks, a fair lessening in the slope of the load-deflection curve was seen and this slope remained linear until yield point of the steel reinforcement. This type of load-deflection behavior of PSCC beam is similar to the lightweight concrete beams investigated by other researchers (Gunasekaran et al., 2013; Mohammed et al., 2014; Teo et al., 2006b). In Table 4.5, there is a comparison shown between the theoretical deflections at mid-span under service load with the experimental deflections. The theoretical deflection is determined from the beam curvatures according to EC2 (2004). In Table 4.5, it can be found that the experimental deflection at the service load is lower than that of theoretical deflection. In a specific manner, experimental deflection is 2-26% lower than the theoretical values.
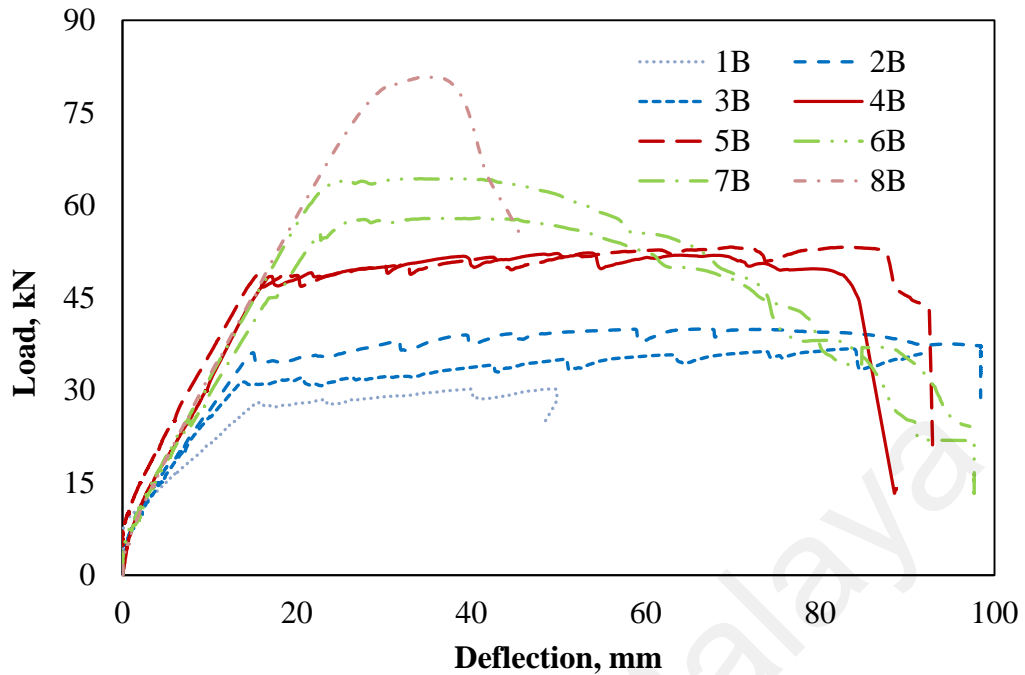
Figure 4.11: Experimental load-deflection curve

In this study, PSCC is found with the lower value of modulus of elasticity. The deflection is governed by the stiffness of concrete beam which directly depends on the modulus of elasticity. Hence, it is reasonable that the deflection of PSCC is large. However, according to EC2 (2004), deflections of beams containing lower reinforcement ratio are still acceptable as the span-deflection ratio ranged from 252 to 335. On the other contrary, span-deflection ratios of beams containing higher reinforcement ratio are ranged from 178 to 209. Therefore, it is being suggested that the larger beam depths should be considered for the higher reinforcement ratio. However, to get a complete understanding of the deflection behavior, additional studies including the effects of creep and shrinkage on the PSCC beam are required.

Table 4.5: Deflection of reinforced PSCC beam at service load

Beam ID	Theoretical service moment, (kN-m)	Experimental deflection, Δ_{exp} (mm)	Theoretical deflection (EC2), Δ_{theo} (mm)	$\Delta_{exp}/ \Delta_{theo}$	Span/Δ_{exp}
1B	10.4	8.1	9.6	0.84	370
2B	14.9	9.5	9.6	0.98	317
3B	14.9	8.9	10.5	0.85	336
4B	22.0	10.3	14.0	0.74	291
5B	22.0	11.9	13.7	0.87	252
6B	25.7	15.8	15.2	1.04	189
7B	25.7	14.4	16.9	0.85	209
8B	41.9	16.9	20.5	0.82	178

4.4.3 Moment capacity

The comparison between the experimental ultimate moment (M_{exp}) and the theoretical design moment (M_{theo}) of tested beam samples has been illustrated in Figure 4.12. Theoretical design moments of the beams are calculated from the rectangular stress block analysis in according with EC2 (2004). From the Figure 4.12, it is clear that the moment capacity of tested beams containing reinforcement ratio up to 1.30% is similar to the theoretical prediction. But for higher reinforcement ratio (2.11%) experimental value is less than the theoretical value. For the optimum prediction of moment carrying capacity, Whitney's (Whitney, 1937) rectangle stress block factor may need to be modified for the PSCC beam with higher reinforcement.
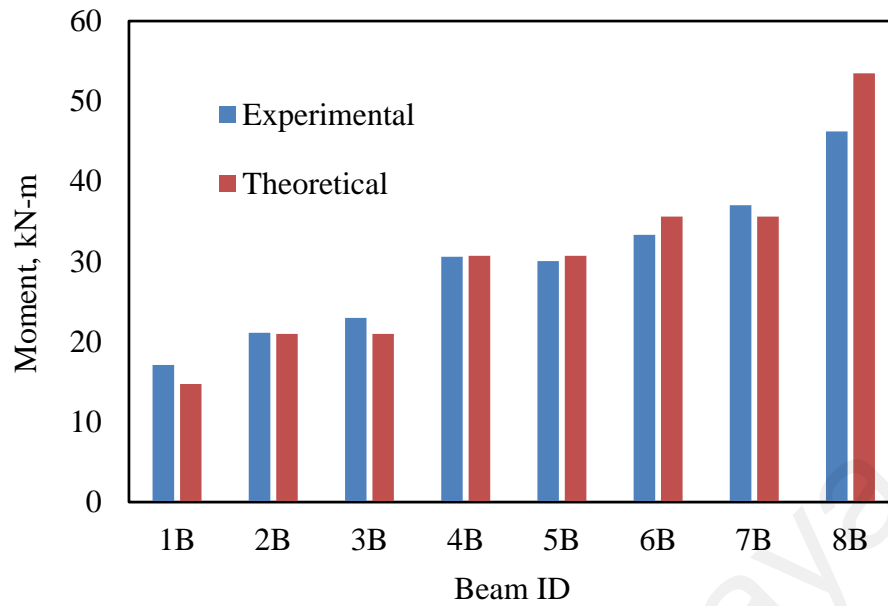
Figure 4.12: Comparison between experimental and theoretical ultimate moment.

4.4.4 First cracking Load

Figure 4.13 shows the comparison between experimental and theoretical first cracking moment. The first cracking moments are found about 38% to 51% of the theoretical first cracking moments. The first cracking moment is considered as a point where an immediate change of initial slope of the moment-deflection curve takes place. Load deflection curve of this research confirms the initial slope change (Figure 4.11). The modulus of rupture overestimates the experimental first cracking moments. Therefore, it is being suggested that about 50% reduced value of modulus of rupture may be used to calculate the cracking moment accurately.
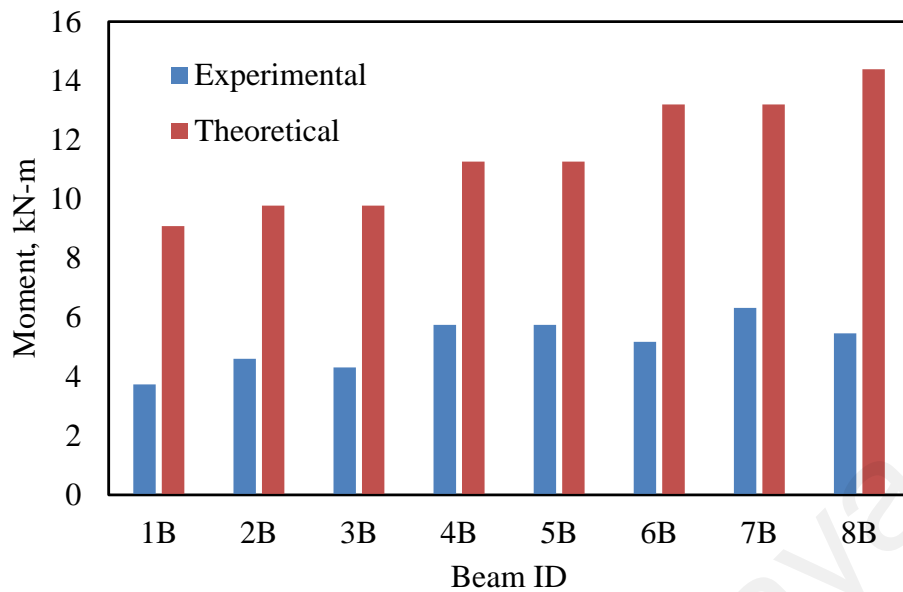
Figure 4.13: Comparison between experimental and theoretical 1st cracking moment

4.4.5 Cracking pattern

Crack widths were recorded at every step of load increment at the tension reinforcement level and the propagations of cracks were marked on the beam. It was observed that first crack always forms near the mid-span of the beam. The cracks at the surface of the PSCC beams were mostly vertical, suggesting a failure in flexure. Table 4.6 shows the cracking feature of the PSCC beams tested.

Table 4.6: Cracking characteristics of reinforced PSCC beam

Beam ID	Theoretical crack width (EC2), (mm)	Experimental crack width service load (mm)	Experimental crack/ Theoretical crack	Experimental crack width failure load (mm)	Average crack spacing (mm)	No. of cracks between loading points
1B	0.16	0.17	1.06	1.33	100	9
2B	0.22	0.21	0.95	1.13	116	6
3B	0.22	0.26	1.18	1.27	111	5
4B	0.20	0.23	1.15	0.94	102	7
5B	0.20	0.26	1.30	0.86	94	7
6B	0.24	0.25	1.04	0.81	101	8
7B	0.24	0.23	0.96	0.77	95	7
8B	0.27	0.28	1.04	0.64	80	10

Table 4.6 shows a comparison of the predicted crack width according to EC2 under service loads with the experimental crack width. For members protected against weather, EC2 permits crack widths up to 0.30 mm. It was observed that EC2 (2004) provides a close prediction for the crack width.

The PSCC beams show the average crack spacing ranged from 94 mm to 116 mm and this pattern is similar to the lightweight aggregate concrete beam made of OPS, POC, and expanded shale (Swamy and Ibrahim, 1975).

4.5   Strain and ductility performance of reinforced PSCC beam

4.5.1   Steel and concrete strain

The steel and concrete strains of the PSCC beam specimens at mid-span are measured with strain gauges up to the failure load. Figure 4.14 represents the steel and concrete strain distribution for the PSCC beam specimens. The steel and concrete strains are found 1760×10^{-6} and 1960×10^{-6} at the service load condition respectively. The measured steel and concrete strains just prior to failure are 4299×10^{-6} and 4268×10^{-6} respectively. It is worth mentioning that the actual strain values must be higher than reported here as the strain readings are recorded up to the 90% of the failure load. However, the test result is in good agreement with the works of previous researchers (Swamy and Lambert, 1984; Teo et al., 2006b). From the above discussion, it can be said that PSCC beam can reach to its full strain capacity under the flexural loading.
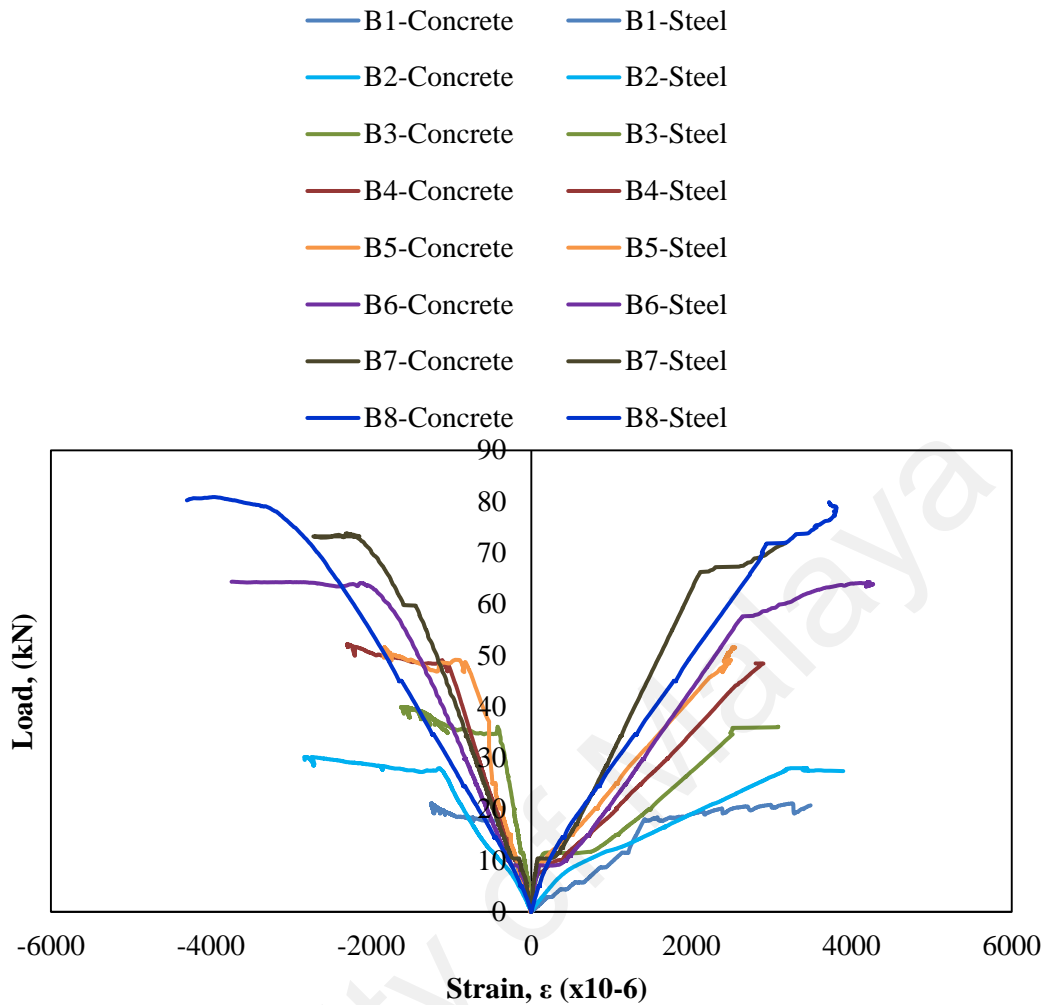
Figure 4.14: Concrete and steel strain of PSCC beam

4.5.2 Sectional strain characteristics

The sectional strain of the PSCC beam at midspan is measured using demec gauge. Demec reading is recorded up to the service load condition. The beam depth (h) versus strain of the PSCC beam specimens for various load level is shown in Figure 4.15. From the figure, it can be seen that strains of all the beams increase with the increase of load. As the strain of the beams recorder up to the service load condition, the materials strain remain up to the elastic range. Therefore, the figure indicates that the neutral axis depth and the strain propagation for all the beams are almost similar. Finally, the beam samples fail with steel yielding hereafter concrete crushing occurs.

Figure 4.15: Sectional strain variation at mid-span of PSCC beam

4.5.3 Ductility characteristics

Ductility of any reinforced concrete element has the supreme significance. Because any ductile element must be able to show the large deflections at ultimate load carrying capacity which ensures the sufficient amount of warning to its failure. Table 4.7 shows the ductility indices of the tested PSCC beams in this study.
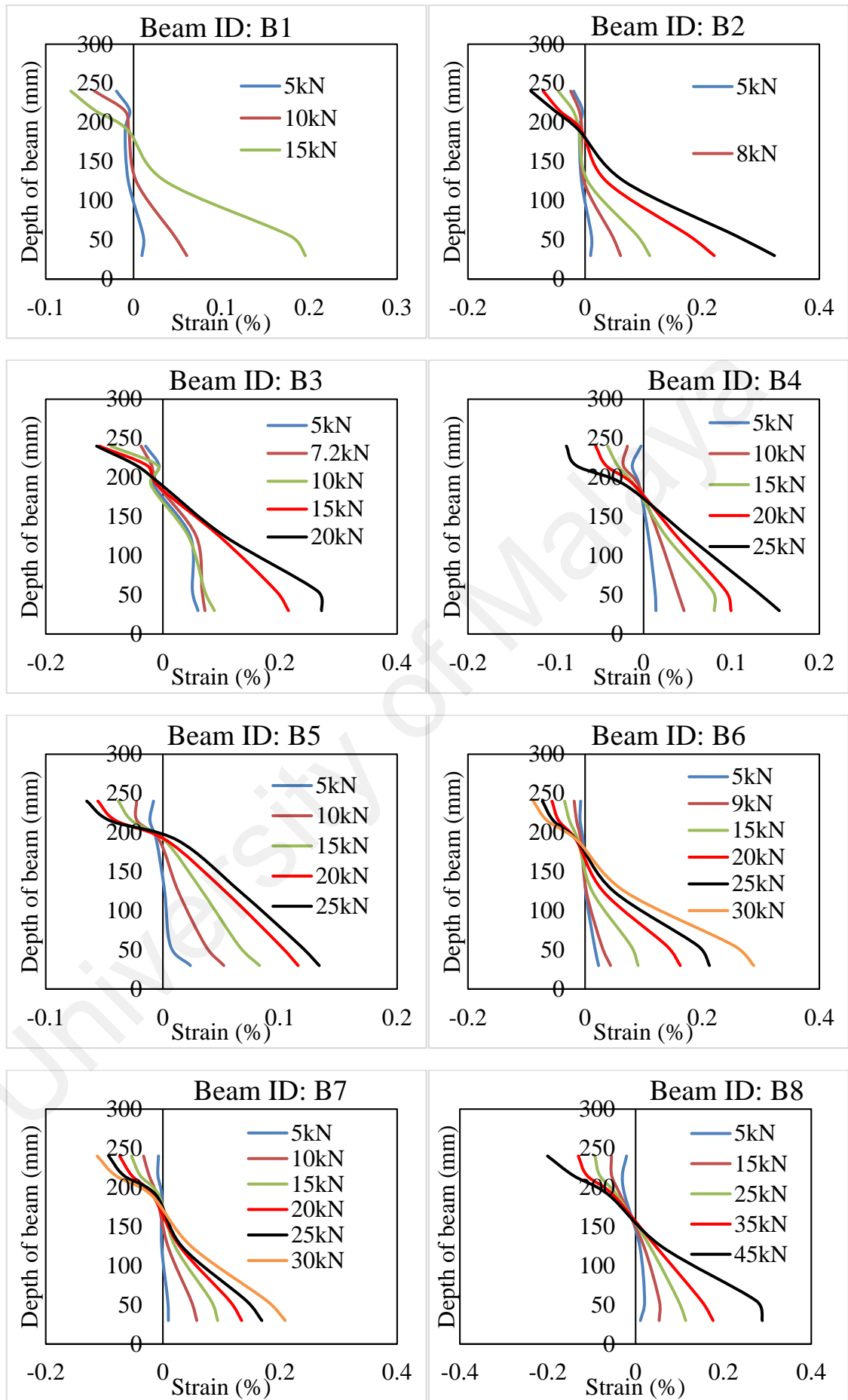
Table 4.7: Displacement ductility of PSCC beams

Beam ID	Yield stage		Ultimate stage		Displacement ductility index, $\mu=\Delta_u/\Delta_y$
	Moment, KN-m	Deflection, Δ_y (mm)	Moment, kN-m	Deflection, Δ_u (mm)	
1B	15.82	15.78	17.11	49.88	3.16
2B	17.76	17.79	21.12	76.30	4.29
3B	20.56	16.86	22.97	73.09	4.34
4B	27.93	15.34	30.61	69.93	4.56
5B	27.58	16.50	30.06	76.99	4.67
6B	31.88	22.65	33.33	46.30	2.04
7B	36.45	23.77	37.04	47.20	1.99
8B	45.00	29.26	46.24	37.22	1.27

The displacement ductility ratio is measured in terms of the ratio of ultimate deflection to yield deflection ($\mu = \Delta_u / \Delta_y$), where Δ_u stands for the deflection at the ultimate moment and Δ_y stands for the deflection at yield. By and large, structural member can undergo enormous deflections before failure if ductility ratio is higher. For the beams with reinforcement ratios up to 1.09%, the ductility ratio was more than 4.29, which indicates a decent ductility. One of the aspects contributing to the good ductility behavior of the PSCC beams was the toughness and good shock absorbance properties of the OPS and POC aggregates as specified by the aggregate impact value (AIV) from Table 3.1. Members with the displacement ductility ratios in the range of 3 to 5 can be taken for structural elements subjected to vast displacements (Ashour, 2000). From this study, it was also found that a higher tension reinforcement ratio (2.11%) results in less

ductile behavior. This is in agreement with the work of other researchers (Lee and Pan, 2003; Rashid and Mansur, 2005).

CHAPTER 5: CONCLUSIONS AND RECOMMENDATIONS

The findings on the engineering properties of PSCC and behavior of the PSCC beam are summarized in this chapter. Several recommendations for future study are also presented.

5.1   Conclusions

From the experimental study, the main conclusions that can be drawn are given below.

5.1.1   Engineering properties of PSCC

i.   450 kg/m^3 cement content can be used for the PSCC mixes which is the lowest among recent studies to produce high strength lightweight concrete.

ii.   The PSCC mixes can produce lightweight concrete with the oven-dry densities less than 2000 kg/m^3 which fulfilled the requirements of lightweight concrete.

iii.   The mix comprising 50% OPS and 50% POC aggregate can be termed as optimum mix. It produces the 28-day compressive strength of 46 MPa which is the highest among the mixes. The regression analysis between the compressive strength of PSCC and UPV showed good linear correlation ($R^2 = 0.8981$).

iv.   The optimum mix gave the highest splitting tensile and flexural strengths among the mixes.

v.   The moduli of elasticity of PSCC mixes were found to be greater than 10 GPa. Most lightweight concrete have moduli of elasticity similar to this.

5.1.2   Stress-strain behavior and ductility performance of PSCC

i.   The strains at the maximum stress of the PSCC samples are in good agreement with the recent study of lightweight aggregate concrete. More specifically, PSCC has the strain value in the range of 0.0028 to 0.0040 at the maximum stress. Poisson's ratio is also in good agreement with the concrete requirement, and the value is 0.21.

ii.   The PSCC samples showed better ductile behavior. The ductility index decreased with the increase of porous POC aggregate content in the concrete mixes.

5.1.3   Flexural behavior of reinforced PSCC beam

i.   All PSCC beams showed typical flexural performance under four point bending. Yielding of the tensile reinforcement took place before crushing of the concrete (compression face) in the pure bending zone.

ii.   The moment capacity of the tested beams was found to be similar to the theoretical prediction by the EC2.

iii.   The deflection under the design service loads for the PSCC beams with lower reinforcement ratio were within the allowable limit provided by EC2. The deflection of beams with higher reinforcement ratios exceeded the deflection limit.

iv. The experimental first cracking moments were found to be less than theoretical first cracking moments ranging from about 38% to 51%.

v. The crack widths of PSCC beams at service loads varied from 0.17 mm to 0.28 mm and this value is within the allowable limit as defined by EC2.

5.1.4 Strain and ductility performance of reinforced PSCC beam

i. Maximum concrete and steel strain of PSCC beam have been found 4299×10^{-6} and 4268×10^{-6} at their failure load, respectively. This confirms that PSCC beam can attain full strain under the flexural loading.

ii. The ductility index for the PSCC beams with reinforcement ratio up to 1.09% is in the range of 3.16 to 4.67.

5.2 Recommendations

PSCC concrete is still of great interest. As the proposed concrete has huge potential in the construction industry, further research should be carried out for gaining full confidence. Following are the important recommendations for future study.

i. Extended studies on all the durability properties of the PSCC at later ages have to be carried out since this research only dealt with engineering properties.

ii. Further investigation is recommended to understand the shear behavior of reinforced PSCC beam.

iii. To obtain a complete understanding of the deflection behavior of PSCC beam, further investigations incorporating the effects of creep and shrinkage on the concrete are required

iv. It is also vital to carry out the experimental and numerical investigations regarding other types of structural members of PSCC, such as reinforced slab and column so as to provide a complete study of the reinforced concrete member behavior which could enhance the applicability of such concrete in the construction industry.

v. It is also envisaged the construction, continuous monitoring and analyzing of large scale reinforced PSCC members in actual structures to enhance the confidence in the utilization of such concrete in the near future.

REFERENCES

Abdullah, A. (1996). Palm oil shell aggregate for lightweight concrete. *Waste material used in concrete manufacturing*, 624-636.

ACI Committee 211.2. (1998). Standard Practice for Selecting Proportions for Structural. Lightweight Concrete *ACI Journal Proceedings, 64*(8).

Ahmad, S. H., Xie, Y., & Yu, T. (1995). Shear ductility of reinforced lightweight concrete beams of normal strength and high strength concrete. *Cement and Concrete Composites, 17*(2), 147-159. doi:http://dx.doi.org/10.1016/0958-9465(94)00029-X

Ahmed, E., & Sobuz, H. R. (2011). Flexural and time-dependent performance of palm shell aggregate concrete beam. *KSCE Journal of Civil Engineering, 15*(5), 859-865.

Ahmmad, R., Jumaat, M., Bahri, S., & Islam, A. S. (2014). Ductility performance of lightweight concrete element containing massive palm shell clinker. *Construction and Building Materials, 63*, 234-241.

Al-Khaiat, H., & Haque, M. (1998). Effect of initial curing on early strength and physical properties of a lightweight concrete. *Cement and Concrete Research, 28*(6), 859-866.

Alengaram, Jumaat, M. Z., & Mahmud, H. (2008). Ductility behaviour of reinforced palm kernel shell concrete beams. *European Journal of Scientific Research, 23*(3), 406-420.

Alengaram, Jumaat, M. Z., Mahmud, H., & Fayyadh, M. M. (2011a). Shear behaviour of reinforced palm kernel shell concrete beams. *Construction and Building Materials, 25*(6), 2918-2927. doi:http://dx.doi.org/10.1016/j.conbuildmat.2010.12.032

Alengaram, Mahmud, H., & Jumaat, M. Z. (2011b). Enhancement and prediction of modulus of elasticity of palm kernel shell concrete. *Materials & Design, 32*(4), 2143-2148.

Alengaram, U., Jumaat, M., & Mahmud, H. (2008). Influence of cementitious materials and aggregates content on compressive strength of palm kernel shell concrete. *J Appl Sci, 8*(18), 3207-3213.

Alengaram, U. J., Mahmud, H., Jumaat, M. Z., & Shirazi, S. (2010). Effect of aggregate size and proportion on strength properties of palm kernel shell concrete. *International Journal of the Physical Sciences, 5*(12), 1848-1856.

Ashour, S. A. (2000). Effect of compressive strength and tensile reinforcement ratio on flexural behavior of high-strength concrete beams. *Engineering Structures, 22*(5), 413-423.

ASTM-C-330-89. (1989). Standard specification for lightweight aggregates for structural concrete. *Annual Book of ASTM Standards*.

ASTM-C-331-89. (1989). Standard specification for lightweight aggregates for masonry concrete. *Annual Book of ASTM Standards*.

ASTM-C-332-87. (1989). Standard specification for lightweight aggregates for insulation concrete. *Annual Book of ASTM Standards*.

Basri, H., Mannan, M., & Zain, M. (1999). Concrete using waste oil palm shells as aggregate. *Cement and Concrete Research, 29*(4), 619-622.

BS8110. (1997). Structural use of concrete. Part I: Code of practice for design and construction. *British Standards Institution, UK*.

BS, Part,116:. (1997). Method for determination of compressive strength of concrete cubes. London: British Standard Institution.

CEB/FIP. (1977). Lightweight Aggregate Concrete. CEB-FIP Manual of Design and Technology: The Construction Press, London.

Chandra, S., & Berntsson, L. (2002). *Lightweight aggregate concrete*: Elsevier.

Chen, B., & Liu, J. (2005). Contribution of hybrid fibers on the properties of the high-strength lightweight concrete having good workability. *Cement and Concrete Research, 35*(5), 913-917.

Choong, M. Y. (2012). Waste not the palm oil biomass. *The Star Online*.

EC2. (2004). 1-2: 2004 Eurocode 2: Design of concrete structures-Part 1-2: General rules-Structural fire design. *European Standards, London*.

Gesoğlu, M., Özturan, T., & Güneyisi, E. (2004). Shrinkage cracking of lightweight concrete made with cold-bonded fly ash aggregates. *Cement and Concrete Research, 34*(7), 1121-1130.

Gunasekaran, K., Annadurai, R., & Kumar, P. (2013). Study on reinforced lightweight coconut shell concrete beam behavior under flexure. *Materials & Design, 46*, 157-167.

Hilton, M., Mohd, S., & Mohd Noor, N. (2007). Mechanical properties of palm oil clinker concrete.

Holm, T. A., & Bremner, T. W. (2000). *State-of-the-art report on high-strength, high-durability structural low-density concrete for applications in severe marine environments*: US Army Corps of Engineers, Engineer Research and Development Center.

Hossain, K. M. A. (2004). Properties of volcanic pumice based cement and lightweight concrete. *Cement and Concrete Research, 34*(2), 283-291.

Hussein, S. H., Mustapha, K., Muda, Z. C., & Budde, S. (2012). Modelling of ultimate load for lightweight palm oil clinker reinforced concrete beams with web openings using response surface methodology. *International Journal of Civil Engineering and Technology, 3*(1), 33-44.

Jang, H.-S., Lim, Y.-T., So, H.-S., & So, S.-Y. (2015). A Study on the Black Colored Expression Properties and Physical Properties of Cement Mortar Using Granulated Blast Furnace Slag. *Science of Advanced Materials, 7*(1), 63-67.

Jumaat, M. Z., Alengaram, U. J., & Mahmud, H. (2009). Shear strength of oil palm shell foamed concrete beams. *Materials & Design, 30*(6), 2227-2236.

Kanadasan, J., & Razak, H. A. (2014). Mix design for self-compacting palm oil clinker concrete based on particle packing. *Materials & Design, 56*, 9-19.

Kılıç, A., Atiş, C. D., Yaşar, E., & Özcan, F. (2003). High-strength lightweight concrete made with scoria aggregate containing mineral admixtures. *Cement and Concrete Research, 33*(10), 1595-1599.

Kockal, N. U., & Ozturan, T. (2011). Strength and elastic properties of structural lightweight concretes. *Materials & Design, 32*(4), 2396-2403.

Kosmatka, S. H., Panarese, W. C., & Association, P. C. (2002). Design and control of concrete mixtures.

Koya, O., & Fono, T. (2009). Palm Kernel Shell in the manufacture of Automotive brake pad: Technoexpo.

Lee, T.-K., & Pan, A. D. (2003). Estimating the relationship between tension reinforcement and ductility of reinforced concrete beam sections. *Engineering structures, 25*(8), 1057-1067.

Leslie, J., & Cheesman, W. (1949). An ultrasonic method of studying deterioration and cracking in concrete structures. *Journal of the American Concrete Institute, 21*(1), 17-36.

Lo, Cui, H., & Li, Z. (2004a). Influence of aggregate pre-wetting and fly ash on mechanical properties of lightweight concrete. *Waste Management, 24*(4), 333-338.

Lo, Cui, H. Z., & Li, Z. G. (2004b). Influence of aggregate pre-wetting and fly ash on mechanical properties of lightweight concrete. *Waste Management, 24*(4), 333-338. doi:http://dx.doi.org/10.1016/j.wasman.2003.06.003

Lopez, M., Kurtis, K., & Kahn, L. (2006). Pre-wetted lightweight coarse aggregate reduces long-term deformations of high-performance lightweight concrete. *ACI Special Publication, 234*.

Mahmud, H. (2010). Mix design and mechanical properties of oil palm shell lightweight aggregate concrete: a review. *International Journal of the Physical Sciences, 5*(14), 2127-2134.

Mannan, M., Alexander, J., Ganapathy, C., & Teo, D. (2006). Quality improvement of oil palm shell (OPS) as coarse aggregate in lightweight concrete. *Building and Environment, 41*(9), 1239-1242.

Mannan, M., & Ganapathy, C. (2001a). Long-term strengths of concrete with oil palm shell as coarse aggregate. *Cement and Concrete Research, 31*(9), 1319-1321.

Mannan, M., & Ganapathy, C. (2001b). Mix design for oil palm shell concrete. *Cement and Concrete Research, 31*(9), 1323-1325.

Mannan, M., & Ganapathy, C. (2004). Concrete from an agricultural waste-oil palm shell (OPS). *Building and Environment, 39*(4), 441-448.

Mannan, M., & Neglo, K. (2010). Mix design for oil-palm-boiler clinker (OPBC) concrete. *Journal of Science and Technology (Ghana), 30*(1).

Mannan, M. A., & Ganapathy, C. (2002). Engineering properties of concrete with oil palm shell as coarse aggregate. *Construction and Building Materials, 16*(1), 29-34.

Mehta, P. K., & Monteiro, P. J. (2006). *Concrete: microstructure, properties, and materials* (Vol. 3): McGraw-Hill New York.

Mo, K. H., Alengaram, U. J., & Jumaat, M. Z. (2014a). A review on the use of agriculture waste material as lightweight aggregate for reinforced concrete structural members. *Advances in Materials Science and Engineering, 2014*.

Mo, K. H., Yap, K. K. Q., Alengaram, U. J., & Jumaat, M. Z. (2014b). The effect of steel fibres on the enhancement of flexural and compressive toughness and fracture characteristics of oil palm shell concrete. *Construction and Building Materials, 55*, 20-28. doi:10.1016/j.conbuildmat.2013.12.103

Mohammed, B. S., Al-Ganad, M. A., & Abdullahi, M. (2011). Analytical and experimental studies on composite slabs utilising palm oil clinker concrete. *Construction and Building Materials, 25*(8), 3550-3560. doi:http://dx.doi.org/10.1016/j.conbuildmat.2011.03.048

Mohammed, B. S., Foo, W., & Abdullahi, M. (2014). Flexural strength of palm oil clinker concrete beams. *Materials & Design, 53*, 325-331.

Mohammed, B. S., Foo, W., Hossain, K., & Abdullahi, M. (2013). Shear strength of palm oil clinker concrete beams. *Materials & Design, 46*, 270-276.

Muda, Z., Sharif, S. F., & Hong, N. J. (2012). Flexural behavior of lightweight oil palm shells concrete slab reinforced with geogrid. *International Journal of Scientific & Engineering Research, 3*(11).

Neville, A. (2008). Properties of concrete CTP-VVP: Malaysia.

Neville, A., & Brooks, J. (2008). Concrete Technology: Malaysia: Prentice Hall.

Neville, A. M. (1970). Hardened concrete: physical and mechanical aspects. *American Concrete Institute Monograph, Monograph 6, 270 PP*.

Neville, A. M. (1995). *Properties of concrete*. England: Pearson Education Limited.

Newman, J., & Choo, B. S. (2003). *Advanced Concrete Technology 3: Processes*: Butterworth-Heinemann.

Newman, J., & Owens, P. (2003). *Properties of lightweight concrete*: Butterworth-Heinemann.

Okafor, F. O. (1988). Palm kernel shell as a lightweight aggregate for concrete. *Cement and Concrete Research, 18*(6), 901-910.

Okafor, F. O. (1991). An investigation on the use of superplasticizer in palm kernel shell aggregate concrete. *Cement and Concrete Research, 21*(4), 551-557.

Okpala, D. (1990). Palm kernel shell as a lightweight aggregate in concrete. *Building and Environment, 25*(4), 291-296.

Omar, & Mohamed, N. (2002). The performance of pretensioned prestressed concrete beams made with lightweight concrete. *Jurnal Kejuruteraan Awam, 14*(1), 60-70.

Raithby, K., & Lydon, F. (1981). Lightweight concrete in highway bridges. *International Journal of Cement Composites and Lightweight Concrete, 3*(2), 133-146.

Rashid, M. A., & Mansur, M. A. (2005). Reinforced high-strength concrete beams in flexure. *ACI Structural Journal, 102*(3).

Rossignolo, J. A., Agnesini, M. V., & Morais, J. A. (2003). Properties of high-performance LWAC for precast structures with Brazilian lightweight aggregates. *Cement and Concrete Composites, 25*(1), 77-82.

Salam, S., Ali, A., & Abdullah, A. (1985). Lightweight concrete using oil palm shells as aggregates.

Shafigh, P., Jumaat, M., Mahmud, H., & Alengaram, U. (2011a). A new method of producing high strength oil palm shell lightweight concrete. *Materials & Design, 32*(10), 4839-4843. doi:http://dx.doi.org/10.1016/j.matdes.2011.06.015

Shafigh, P., Jumaat, M. Z., & Mahmud, H. (2011b). Oil palm shell as a lightweight aggregate for production high strength lightweight concrete. *Construction and Building Materials, 25*(4), 1848-1853.

Shafigh, P., Mahmud, H. B., & Jumaat, M. Z. (2012). Oil palm shell lightweight concrete as a ductile material. *Materials & Design, 36*, 650-654.

Shannag, M. J. (2000). High strength concrete containing natural pozzolan and silica fume. *Cement and Concrete Composites, 22*(6), 399-406. doi:http://dx.doi.org/10.1016/S0958-9465(00)00037-8

Shannag, M. J. (2011). Characteristics of lightweight concrete containing mineral admixtures. *Construction and Building Materials, 25*(2), 658-662.

Shetty, M. (2005). *Concrete technology theory and practice. 1rd Multicolor illustrative revised ed*: India.

Short, A., & Kinniburgh, W. (1978). *Lightweight concrete*: Applied Science Publishers London.

Swamy, R., & Ibrahim, A. (1975). Flexural behaviour of reinforced and prestressed Solite structural lightweight concrete beams. *Building Science, 10*(1), 43-56.

Swamy, R., & Lambert, G. (1984). Flexural behaviour of reinforced concrete beams made with fly ash coarse aggregates. *International Journal of Cement Composites and Lightweight Concrete, 6*(3), 189-200.

Sylva, G., Burns, N., & Breen, J. (2004). Composite bridge systems with high-Performance lightweight concrete. *ACI Special Publication, 218*.

Teo, D., Mannan, M., & Kurian, V. (2006a). Structural behaviour of singly reinforced OPS beams.

Teo, D., Mannan, M. A., & Kurian, J. V. (2006b). Flexural behaviour of reinforced lightweight concrete beams made with oil palm shell (OPS). *Journal of Advanced Concrete Technology, 4*(3), 459-468.

Teo, D., Mannan, M. A., Kurian, V., & Ganapathy, C. (2007). Lightweight concrete made from oil palm shell (OPS): structural bond and durability properties. *Building and Environment, 42*(7), 2614-2621.

Teo, D., Mannan, M. A., & Kurian, V. J. (2006c). Structural concrete using oil palm shell (OPS) as lightweight aggregate. *Turkish Journal of Engineering and Environmental Sciences, 30*(4), 251-257.

Turatsinze, A., & Garros, M. (2008). On the modulus of elasticity and strain capacity of self-compacting concrete incorporating rubber aggregates. *Resources, conservation and recycling, 52*(10), 1209-1215.

Whitney, C. S. (1937). *Design of reinforced concrete members under flexure or combined flexure and direct compression.* Paper presented at the ACI Journal Proceedings.

Wiegrink, K., Marikunte, S., & Shah, S. P. (1996). Shrinkage cracking of high-strength concrete. *ACI Materials Journal, 93*(5).

Wilson, H., & Malhotra, V. (1988). Development of high strength lightweight concrete for structural applications. *International Journal of Cement Composites and Lightweight Concrete, 10*(2), 79-90.

APPENDIX A: TEST RESULTS FOR STEEL PROPERTIES

A.1 Steel Properties

Tensile Test
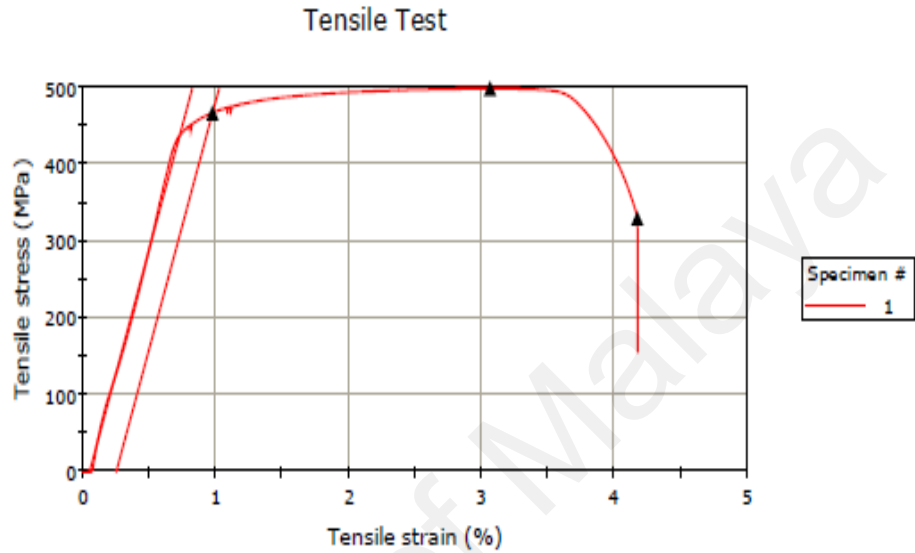
	Specimen Name	Max Load (kN)	Maximum Stress (MPa)	Break Load (kN)	Extension at Break (mm)	Modulus (MPa)	Stress at 0.2% Yield (MPa)	Comments
1	r1-6mm	14.079	497.952	9.324	14.608	64,317.970	466.324	16/5/12
Mean		14.079	497.952	9.324	14.608	64,317.970	466.324	
Std Dev		-----	-----	-----	-----	-----	-----	
Coeff Var		-----	-----	-----	-----	-----	-----	

B.1 Moment capacity of PSCC beam

The moment capacity of PSCC beam has been calculated according to EC2. Load capacity is obtained from the moment capacity.

$$F_c = \frac{\alpha f_{ck}}{\gamma_c} \, 0.8xb$$

Where,

$\alpha = 0.85$

$f_{ck} = 45 \; MPa$

$\gamma = 1.5$

$x = Depth \; of \; neutral \; axis$

$$F_s = \frac{A_s f_y}{\gamma_s}$$

Where,

$A_s = 226 \; mm^2$

$f_y = 466 \; MPa$

$\gamma_s = 1.15$

$$\varepsilon_s = (\frac{d-x}{x})\varepsilon_{ult}$$

Where,

$\varepsilon_s = Steel \; strain$

$\varepsilon_{ult} = Ultimate \; strain \; of \; concrete$

$$F_c = \frac{0.85 \times 45}{1.5} \times 0.8 \times x \times 150$$

$$F_s = \frac{226 \times 466}{1.15}$$

Thus $x = 22.71\ mm$

$\varepsilon_{ult} = 0.003\ (Assumed)$

Hence $\varepsilon_s = 0.025 > 0.002$

So reinforcement has yielded.

$$M_{ult} = F_s(d - 0.44x) = 18.90\ kN - m$$

$$P = \frac{2 \times M_{ult}}{1.15} = 32.85\ kN$$

LIST OF PUBLICATIONS

1. Md. Nazmul Huda, Mohd Zamin Bin Jumaat and A.B.M. Saiful Islam (2016), "Flexural performance of reinforced oil palm shell & palm oil clinker concrete (PSCC) beam", **Published** in Construction & Building Materials Journal. *Q-1, ISI-Ranked journal*.

2. Md. Nazmul Huda, Mohd Zamin Bin Jumaat and A.B.M. Saiful Islam (2016), "Influence of palm oil factory waste material as coarse aggregate species for high-performance lightweight concrete" **accepted and in press** for publication in Revista de la Construcción. *ISI-Ranked journal*.

3. Md. Nazmul Huda, Mohd Zamin Bin Jumaat, A.B.M. Saiful Islam and Mahmudur Rahman Soeb (2015), "Ductility Performance of High Strength Lightweight Concrete Produced from a Mixture of Oil Palm Shell and Palm Oil Clinker Aggregates", **presented and published** in CICM 2015, First International Conference on Advances in Civil Infrastructure and Construction Materials, MIST, Dhaka, Bangladesh, 14–15 December 2015.

4. Huda, M. N., Jumaat, M. Z. and Islam, A. B. M. S., (2015, 27 May). "Combination of oil palm shell and palm oil clinker for the production of structural lightweight concrete", **Poster presentation,** Engineering Postgraduate Day, Engineering Tower, Faculty of Engineering, University of Malaya, Kuala Lumpur, Malaysia.